Alma Mater Studiorum · Università di Bologna

Scuola di Scienze
Dipartimento di Fisica e Astronomia
Corso di Laurea in Fisica

SCALARIZED BLACK HOLES IN SCALAR GAUSS-BONNET MODELS WITH A POSITIVE COSMOLOGICAL CONSTANT

Relatore:
Prof. Roberto Casadio

Presentata da:
Sara Sanseverinati

Correlatori:
Dott. Alexandre M. Pombo
Dott. Lorenzo Pizzuti

Anno Accademico 2023/2024

Abstract

Since the start of modern Astrophysics and Cosmology, two mysteries have been puzzling researchers: dark energy and dark matter. While many possibilities exist, due to its non-interacting nature – only through the gravitational field – little progress has been made. In order to tackle this, researchers have been trying to get clearer answers through the study of exotic ultra-compact objects and/or alternative gravity models. On the alternative model side, one of the approaches is to consider higher curvature terms and/or bosonic scalar fields. The latter provides a possible explanation for the highly accelerated expansion of the early Universe (inflation) and the non-vanishing cosmological constant at the current times. The theories of modified gravity that include extra scalar fields, so-called scalar-tensor theories, present some interesting phenomenology. An intriguing possibility occurs when the additional scalar field is non-minimally coupled to the gravitational sector. The interaction between a scalar field and the strong spacetime curvature of a black hole (BH) originates what is known as scalarization. The latter endows BHs surrounded by a real scalar field with interesting and distinct characteristics. Alternatively, low-compactness objects that do not have enough curvature can be helped by the presence of a positive cosmological constant, allowing objects like galaxies and galaxy clusters to suffer scalarization, adding an extra mass profile outside of the observable matter. It then follows the possibility of the matter profile coming from the scalarized low-density objects in the presence of a cosmological constant to mimic the observed dark matter. For this study, we will consider scalarized objects in an extended scalar-tensor theory where the scalar field is non-minimal coupled through a quartic coupling function to the Gauss-Bonnet invariant and in the presence of a positive cosmological constant. Firstly, the equations of motion for the metric and the scalar field were obtained from the action. Then, through the numerical method Runge-Kutta with a shooting method, the profiles of the scalar field between the Schwarzschild horizon and the cosmological horizon were derived for various values of the coupling constant β and Λ. Finally, plots of β related to the main parameters of the problem have been extracted from the results of the integration and the plots of BH evolutionary branches.

Abstract

Fin dalla nascita dell'Astrofisica e della Cosmologia moderne, due misteri hanno affascinato i ricercatori: l'energia oscura e la materia oscura. Sebbene esistano molte possibilità, a causa della loro natura non interagente – solo attraverso effetti gravitazionali – sono stati fatti pochi progressi. Per affrontare questo problema, i ricercatori hanno cercato di ottenere risposte più chiare attraverso lo studio di oggetti ultra-compatti esotici e/o modelli di gravità alternativi. Nel campo dei modelli alternativi, uno degli approcci è considerare termini di curvatura più elevati e/o campi scalari bosonici. Questi ultimi forniscono una possibile spiegazione per l'espansione accelerata dell'Universo primordiale (inflazione) e il valore non nullo della costante cosmologica ai giorni nostri. Le teorie della gravità modificata che includono campi scalari aggiuntivi, le cosiddette teorie scalari-tensoriali, presentano una fenomenologia interessante. Un'intrigante possibilità si verifica quando il campo scalare aggiuntivo è accoppiato in modo non minimale al settore gravitazionale. L'interazione tra un campo scalare e la forte curvatura dello spaziotempo di un buco nero origina un fenomeno noto come scalarizzazione. Quest'ultima fa sì che i buchi neri risultino circondati da un campo scalare reale con caratteristiche peculiari e distintive. In alternativa, oggetti non così compatti da generare una curvatura sufficiente possono essere aiutati dalla presenza di una costante cosmologica positiva, permettendo a strutture come galassie e ammassi di galassie di subire la scalarizzazione, aggiungendo un profilo di massa extra al di fuori della materia osservabile. Vi è quindi la possibilità che il profilo di materia derivato dagli oggetti a bassa densità scalarizzati grazie alla presenza di una costante cosmologica possa imitare la materia oscura osservata. Per questo studio, considereremo la scalarizzazione che oggetti a bassa densità subiscono nel contesto teorico di una teoria scalare-tensore estesa dove il campo scalare è accoppiato in modo non minimale attraverso una funzione d'accoppiamento di quarto grado all'invariante di Gauss-Bonnet e in presenza di una costante cosmologica positiva. In primo luogo, si sono derivate a partire dall'azione le equazioni del moto per la metrica e il campo scalare. Poi, attraverso il metodo numerico Runge-Kutta con un metodo di shooting, sono stati derivati i profili del campo scalare tra l'orizzonte di Schwarzschild e l'orizzonte cosmologico, per vari valori della costante di accoppiamento β e Λ. Infine, dai risultati dell'integrazione e dai grafici dei rami evolutivi dei buchi neri sono stati estratti i grafici che relazionano β ai principali parametri del problema.

Dedication

With love, to all my family

Acknowledgements

My deepest gratitude goes to Dr. Alexandre M. Pombo and Dr. Lorenzo Pizzuti, without whom this work would not have been possible. I am grateful to them for the great amount of time spent explaining complex and stimulating concepts to me, and for the patience required in the challenging task of supervising and reviewing a work that has represented one of the most demanding challenges of my life. I consider myself lucky for everything I have been able to get out of this work thanks to their supervision. With admiration for the passion and dedication with which they carry out scientific research in such a difficult field, I hope that one day they can be proud of me.

I would like to thank Professor Roberto Casadio for his immediate and kind availability.

I am grateful to all my family for always supporting and encouraging me.

I would like to thank also Federico for these years spent studying together, for bearing with me and supporting me even when I was at my lowest.

Last, but not least, I thank my friends and classmates for giving me moments of lightheartedness even during the most difficult times.

Contents

1 Introduction **4**

2 Classical General Relativity **8**
2.1 Black Holes 16
2.1.1 Schwarzschild solution 18
2.1.2 Reissner-Noström solution 21
2.1.3 Kerr-Newmann solution 22

3 Beyond GR **25**
3.1 Lovelock's theorem 25
3.2 Ostrogradsky's theorem 27
3.3 Scalar Fields 28
3.3.1 Scalarization 30
3.4 Gauss-Bonnet Scalar-Tensor theory 33
3.4.1 Setting the equations 33
3.4.2 Obtaining solutions 36

4 Conclusion **47**

Chapter 1

Introduction

Since its formulation in 1915, Einstein's General Relativity (GR) has successfully predicted numerous phenomena such as gravitational redshift [32], gravitational deflection of light [90], and perihelion precession of Mercury [91]. On the strong gravity regime, recent gravitational wave detection from ground-base interferometers (*e.g.* the LIGO-VIRGO collaboration [2]) and the observations from the Event Horizon Telescope (EHT) collaboration [28] have indicated a population of extremely compact objects, known as black holes (BH), at different mass scales, and confirmed the existence of gravitational waves, as predicted by GR [31]. Such objects provide a natural "laboratory" to probe and test the strong gravity regime, whereas it would have been impossible to do on Earth or at the Solar System scale.

Nowadays, observational and theoretical reasons have led to the question of whether GR is the complete theory of gravity [86]. While GR describes gravity, the Standard Model unfolds the other three fundamental interactions, strong, electromagnetic, and weak interactions, unifying these last two. On one side there is GR, the classical theory of gravity that however ignores quantum physics aspects. On the other side, the Standard Model of particle physics is a quantum field theory. What is missing, from a theoretical point of view, is a consistent theory of quantum gravity. By trying to describe the gravitational field from a standard quantum field theory perspective, it appears the fact that GR is not a renormalizable theory, making it difficult to quantize gravity. Moreover, it foresees the presence of spacetime singularities such as the ones at the center of BHs, where the laws of physics break down because of the intense gravitational force and infinite curvature of spacetime [43]. Additionally, the standard cosmological model, *aka* ΛCDM model, is based on GR as the theory to describe the gravitational interaction; however, it requires additional components in order to match observational constraints at different scales and environments. For instance, to explain the formation of large-scale structure in the early Universe (*e.g.* [76]), the galaxy rotation curves (*e.g.* [48]) and the anisotropies in the cosmic microwave background (CMB), a collisionless, cold dark matter (CDM) component has been introduced, which should account for the $\sim 26\%$ of

the matter-density budget in the Universe [3]. In addition, the accelerated expansion of the Universe [9, 77] is explained with the presence of a dark energy component (DE), which dominates the cosmological energy-density ($\sim 68\%$). Both CDM and DE are still completely unknown and undetected directly.

In an endeavor to explain the observed Universe, several alternatives/modifications of GR have emerged. According to Lovelock's theorem [58], Einstein's field equations (with a cosmological constant) are the only possible second-order Euler-Lagrange equations derived from a Lagrangian scalar density in four dimensions (4D hereafter) that is constructed solely from the metric. Thus, evading the assumptions of Lovelock's theorem offers many different possibilities for exploring deviations from GR. In this way, an alternative theory of gravity ends up freeing new degrees of freedom. One of these may be to include new, so far undetected, fundamental fields.

In particular, by including scalar fields along with the metric tensor field, one obtains a set of modified gravity theories known as scalar-tensor theories. In this framework, the additional scalar field is dynamical, and non-minimally coupled to the curvature of spacetime. In scalar-tensor theories, the action typically includes a scalar field (ϕ) that couples to the Ricci scalar (R) of the spacetime metric, with a kinetic term and a potential. These theories aim at explaining the observable Universe and address the problem of the cosmological constant (extremely small and yet nonzero), introducing a decaying cosmological "constant" [40].

Extended scalar-tensor theories (ESTTs) are an extension of the previous theories, allowing for more general interactions involving the scalar field and new terms: the Lagrangians contain possible algebraic invariants of second-order with a non-minimal coupled dynamical scalar field. They are at most quadratic in the second derivatives of the scalar field and they allow higher-order equations of motion. This study takes into account extended scalar-tensor-Gauss-Bonnet gravity (ESTGB) where the scalar field is non-minimally coupled to the Gauss-Bonnet invariant (GB) [41]. The latter is a particular combination of curvature terms resulting in a topological invariant in 4D. This means that the integral over a closed manifold of the GB term is a constant characterizing the manifold; however, when the GB invariant is coupled to the scalar field it is able to dynamically contribute to the equation of motion, and so modify the dynamics of gravity. In particular, the GB term is the only second-order curvature correction that leads to equations of motion that are still of second-order, as in GR (and so it does not introduce ghosts, see *e.g.* [73]).

These theories come with a peculiar mechanism that describes the behavior of the scalar field concerning the surrounding large curvature environment. Indeed, while scalar fields are thought to be suppressed in the weak gravity regime (GR is restored), they could be non-vanishing near compact objects. Whenever the curvature of spacetime is strong enough, the coupling of the scalar field to the intense gravitational field - generated by the strong curvature of space-time around compact objects - leads to a phenomenon called scalarization in which, under specific conditions, these compact objects can exhibit

around them a real scalar field. For values of the curvature large enough (above some threshold), the non-minimal coupling of the scalar field and the spacetime curvature becomes stronger and the scalar field could acquire a sufficiently negative effective mass, leading to a *tachyonic* instability. While in physics, the mass squared of a particle or field is usually positive, leading to stable oscillatory behavior, a negative mass squared makes the field experience exponential growth instead of oscillation. This instability indicates a phase transition of the system to a new branch of stable solution characterized by a non-trivial scalar field configuration (see Fig. 1.1).

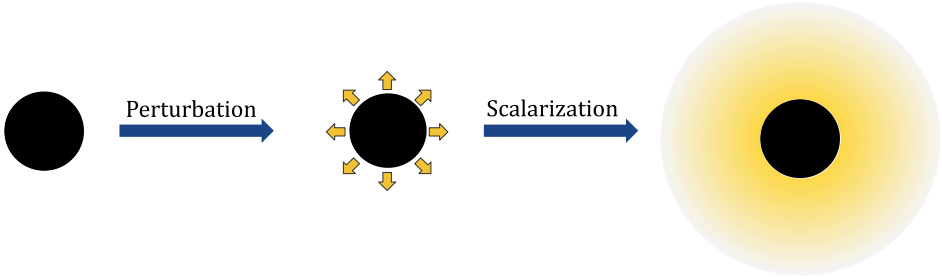

Figure 1.1: Compact objects can exhibit a non-trivial scalar configuration since the extremely high curvature around them triggers scalarization through the non-minimal coupling between the scalar field and curvature term.

In ESTGB, the scalarization mechanism allows for circumventing the no-hair conjecture, which in the framework of GR states that BH can be completely described by only three externally observable classical parameters: mass, electric charge, and angular momentum [83, 53, 12]. In other words, according to GR, no additional "hair" can exist outside the BH event horizon, where "hair" is the colloquial word referring to other information or fields; however, in some modified gravity theories characterized by the presence of higher-curvature terms, such as the quadratic GB invariant, BH can grow "hair" under certain constraints [6, 10]. These constraints are concerned, for example, with the form of the coupling function, leading to different types of scalarization.

In the dilatonic type (Einstein-dilaton-Gauss-Bonnet theory) [85] the form of the coupling function can be linear, $f(\phi) = \alpha\phi$ (α the coupling constant), or exponential, $f(\phi) = \frac{1}{\alpha}(1 - e^{\alpha\phi})$. In this case, a scalar field is always present, BHs always have hair, and they never reduce to the Schwarzschild solution.

In the case of spontaneous scalarization [5, 36] the couplings can be of the form $f(\phi) = \alpha\phi^2$, $f(\phi) = \frac{1}{2\alpha}(1-e^{-\alpha\phi^2})$, and it admits both BH solutions of GR - Schwarzschild vacuum - and hairy BHs - scalarized Schwarzschild. As they are simultaneously present, it is possible to go from vacuum to scalarized solutions thanks to any small perturbation (quantum fluctuations) that enhance the GB curvature invariant. When the GR BH becomes linearly unstable below a certain BH mass, the scalarized solution is preferred. This mechanism resembles a phase transition between two configurations: scalar field

activated under strong-gravity regimes and inefficient in weak-gravity regimes.

Interestingly, non-linear scalarization can also exist. Characterized by non-linear coupling functions such as $f(\phi) = \beta\phi^4$, $f(\phi) = \frac{1}{4\alpha}(1 - e^{\beta\phi^4})$ (even power and higher than 2). In this case, Schwarzschild solutions exist and are always linearly stable, while they are unstable against non-linear (large) perturbations. Non-linear instability leads to the formation of new BHs with scalar hair, and at least two scalarized solutions exist. It is said to be non-linear since this time one needs non-linear, stronger, perturbations to transition to these new branches.

Generalizations of these theories have led to considering the effects of mass and the presence of non-zero potential for the scalar field on the scalarization mechanism and its conditions[75, 62].

Finally, it is also intriguing to study the behavior under a mixture of linear and non-linear, such as it can be $f(\phi) = \alpha\phi^2 + \beta\phi^4$.

While scalarization is a phenomenon that concerns sufficiently compact objects and the high curvature of spacetime they cause (BH and Neutron Star), low-compactness objects can suffer scalarization when helped by a positive cosmological constant. As a consequence, galaxies and galaxy clusters could present an additional mass profile other than the observable matter. There is then the possibility that this additional mass profile from scalarized low-compactness objects in the presence of positive cosmological constant could account for dark matter.

This study follows the scalarization of BHs and searches then for the scalarized cosmological horizon in the framework of ESTGB gravity and a positive cosmological constant. In particular, it has been considered the case of non-linear scalarization with a quartic coupling function $f(\phi) = \beta\phi^4$.

The first section is dedicated to the review of the steps that have led to the formulation of GR and its main concepts. Inside the GR mathematical framework, the most mysterious and exotic prediction of this theory is explored: BHs, from the simplest - non-rotating and uncharged Schwarzschild BH - to the most general solution - rotating and electrically charged Kerr-Newmann BH.

Starting from the second section, the question of how it is possible to overcome GR is addressed: Lovelock's theorem and Ostrogradsky's theorem are stated, followed by a brief presentation of the possible applications of scalar fields in the most recent developments in physics. Regarding scalar fields in the context of modified gravity, it is important to present then the scalarization mechanism.

The field of scalar-tensor theories is vast, but since this study focuses in particular on the ESTGB with a positive cosmological constant, the GB invariant is presented.

The last part of this thesis reports the steps followed to obtain results from this model, from the setting of the equations to their numerical integration. Finally, the main plots that have been obtained are shown, concerning the main parameters of the problem such as the value of the cosmological constant, the radius of the cosmological horizon, and the amplitude of the scalar field.

Chapter 2

Classical General Relativity

Historically speaking, Newton's mechanics and its Galilean Principle of Relativity have been established for decades: "*The laws of (Newtonian) mechanics are the same for all inertial observers*". In Newton's theory, time and space are absolute and separate entities. In addition, gravity is described as a force that acts at a distance and instantaneously between two masses, it is proportional to the product of the masses and inversely proportional to the square of the distance between them. With Newton's gravity, we can successfully explain and predict the orbit of planets and objects on Earth.

In the 19^{th} century Maxwell formulated his theory of electromagnetism, predicting the light to travel at a fixed velocity, denoted with the letter c. However, on one side the theory did not specify any frame of reference in which the laws were valid, on the other the light could not travel at c in every frame of reference according to Galileo's transformations. This question led to the well-known search for the ether, hypothesized to be the privileged frame, even though it was never found. To solve this dilemma, in 1905 Einstein formulated the theory of Special Relativity (SR). This theory is based on two postulates:

- The speed of light in a vacuum is independent of the observer;
- The laws of physics are the same for all inertial observers.

The Galilean Principle of Relativity is thus incompatible: Galilean velocity composition formula would predict unbounded velocities, whereas the speed of light is taken to be fixed in the vacuum. As a consequence, the Galilean transformations were replaced by Lorentz (Poincaré) transformations to relate space and time coordinates when changing from one inertial frame of reference to another: space and time thus merge into a single entity, spacetime; phenomena such as relativity of simultaneity, time dilation, and length contraction arise when moving between different inertial reference frames. Even if simultaneity is relative, with SR Einstein ensured that the cause-effect sequence would

have remained the same in all frames of reference. However, SR also has its limitations: it does not address an accelerating frame of reference, and it does not include gravity.

A turning point in the formulation of GR (as a generalization of the previous one) has been the elaboration of the Einstein Equivalence Principle (EEP[1], known as the famous Einstein's mental experiment of an object inside an elevator): *"Motion in a uniform gravitational field can not be distinguished from free fall"* (see Fig. 2.1). In other words, no local experiment can tell whether the observer is freely falling or is not subjected to any gravitational attraction at all.

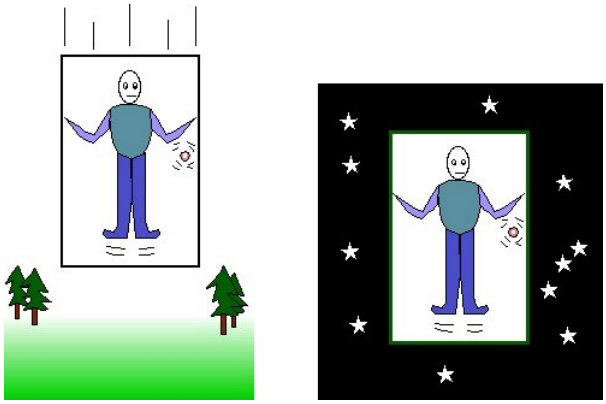

Figure 2.1: Objects falling freely in gravity field all accelerate by the same amount, so they move the same way as if they were in a region of zero gravity - "weightless".

If the effects of gravity seem to vanish in a free fall motion, then the effects experienced in an accelerated frame of reference appear similar to gravity. What we perceive as gravitational force is actually the result of being in a non-inertial (accelerated) frame of reference. It is precisely this close connection between acceleration and gravity that has led to the description of gravity no longer as a force at a distance (Newton's gravity) but rather as a geometric property of spacetime (see Fig. 2.2).

More specifically, gravity is geometrically interpreted as the effect of the curvature of spacetime, and what causes the curvature are mass and energy (they are a source of gravity). In turn, the motion of objects and propagation of light are influenced by how spacetime is curved. Furthermore, GR manages to include every frame of reference (accelerating and inertial) thanks to the mathematical framework of differential geometry *"The laws of physics are the same in all reference frames (for all observers)"*. This implies the mathematical requirement that all physical laws be expressed in terms of

[1]Its precursor is the Equivalence Principle in the Galilean (or Newtonian) form, also known as Weak Equivalence Principle (WEP). It states "For all physical objects, the gravitational charge (mass) m_g equals the inertial mass m_i". This means that every object falls at the same rate in a gravitational field, independent of the composition of the object, as Galileo has demonstrated.

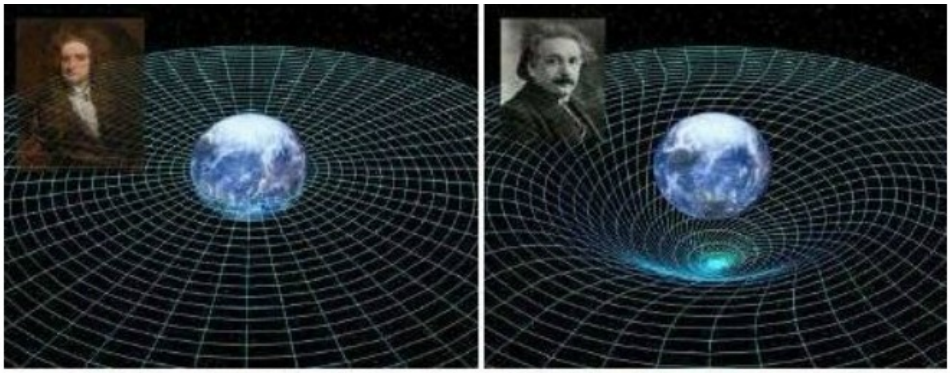

Figure 2.2: Newton described gravity as a force that acts at a distance and instantaneously, while Einstein introduced a geometrical interpretation of gravity as the curvature of spacetime caused by mass and energy

tensor in the sense of differential geometry, so they are covariant under any arbitrary smooth coordinate transformation.

In this way, the formulation of GR must be compatible with SR. The mathematical interpretation of the EEP leads to identifying the free-falling reference frame with the inertial frames of SR. According to SR, physics in these frames must be locally described by tensorial equations in the sense of the local Lorentz group. Then, according to the Principle of General Covariance "*The laws of physics in a general reference frame are obtained from the laws of Special Relativity by replacing tensor quantities of the Lorentz group with tensor quantities of the spacetime manifold*". Practically, this means interpreting tensors under the Lorentz group as tensors under general coordinate transformations, replacing the Minkowski metric of SR with a generic metric tensor and the partial derivative with the metric covariant derivative.

Finally, having set the physical idea under gravitational interaction and the mathematical framework of differential geometry, Einstein's field equations describe how mass and energy distribution curve spacetime:

$$G_{\mu\nu} + \Lambda g_{\mu\nu} = R_{\mu\nu} - \frac{1}{2}Rg_{\mu\nu} + \Lambda g_{\mu\nu} = \frac{8\pi G_N}{c^4}T_{\mu\nu}. \tag{2.1}$$

In the expression above G_N is the gravitational constant, Λ is the cosmological constant, $G_{\mu\nu} = R_{\mu\nu} - \frac{1}{2}Rg_{\mu\nu}$ is the Einstein Tensor, $T_{\mu\nu}$ is the stress-energy tensor, R is the Ricci scalar and $R_{\mu\nu}$ is the Ricci tensor. In particular, the latter are contractions of the Riemann tensor. The characterization of each one is explained below:

- Riemann Tensor ($R_{\mu\nu\rho\delta}$): the Riemann tensor is a $(1,3)$-tensor that defines com-

pletely[2] the curvature of a manifold in a way that is intrinsic (does not need to see manifolds in a larger space and it is independent from the coordinates). Indeed the Riemann tensor uses holonomy to detect curvature. Considering manifolds without torsion (symmetric affine connection and null covariant derivative of the metric tensor) and three vector fields on it, $\vec{W}$, $\vec{V}$, $\vec{A}$, the Riemann tensor is defined as follows:

$$R(\vec{V},\vec{W}) = [\nabla_{\vec{V}}, \nabla_{\vec{W}}]\vec{A} \; . \tag{2.2}$$

Specifically, these objects in differential geometry describe how base vectors transform as they are parallel transported on a manifold. The Riemann tensor defines curvature, in particular, as the effect of the parallel transport of a vector field along a closed loop. Considering on a manifold a closed loop built from two vector fields that commute ($\vec{W}$ and $\vec{V}$ in Eq. 2.2), the Riemann tensor takes the two vector fields that identify the directions of the loop and the parallel transported vector ($\vec{A}$ in Eq. 2.2) as arguments. As a result, it gives a vector that measures how $\vec{A}$ has changed after the parallel transport around that loop. If all its components vanish, $R^{\sigma}_{\mu\nu\rho} = 0$, it means there is no holonomy, the parallelly transported vector has the same orientation between the beginning and the end of the loop, and so the manifold is flat. Otherwise, if there are some non-vanishing components, it indicates the presence of holonomy, meaning the vector does not return to itself due to the curvature of the manifold.

There is also another way the Riemann tensor discloses the curvature of spacetime and it is called geodesic deviation: on curved manifolds, geodesics[3] that are parallel at first naturally come closer or spread out over space. The Riemann tensor measures the relative acceleration between geodesics (how fast they come closer or move away). Therefore, it can be said that the Riemann Tensor completely describes spacetime and how it is curved; it encrypts spacetime shape.

In terms of the affine connection Γ

$$R^{\sigma}_{\mu\nu\rho} = \frac{\partial \Gamma^{\sigma}_{\mu\rho}}{\partial x^{\nu}} - \frac{\partial \Gamma^{\sigma}_{\nu\mu}}{\partial x^{\rho}} + \Gamma^{\sigma}_{\nu\lambda}\Gamma^{\lambda}_{\mu\rho} - \Gamma^{\sigma}_{\rho\lambda}\Gamma^{\lambda}_{\nu\mu} \; . \tag{2.3}$$

The affine connection, also known as Christoffel symbols, is expressed in terms of the inverse metric and first-order partial derivatives of the metric:

$$\Gamma^{\alpha}_{\mu\lambda} = \frac{1}{2} g^{\alpha\nu} \left\{ \frac{\partial g_{\mu\nu}}{\partial x^{\lambda}} + \frac{\partial g_{\lambda\nu}}{\partial x^{\mu}} - \frac{\partial g_{\mu\lambda}}{\partial x^{\nu}} \right\} , \tag{2.4}$$

and $g^{\alpha\nu}$ indicates the inverse of the metric tensor.

[2] All other entities that describe curvature can be obtained from it.

[3] Lines composed by the union of infinitesimal parallel transport of a vector with respect to itself $\nabla_{\vec{V}}\vec{V} = 0$.

- Ricci tensor ($R_{\mu\nu}$): the Ricci tensor is the contraction of the Riemann tensor $R_{\alpha\beta} = \overline{R^{\rho}_{\alpha\rho\beta}}$ (sum over the index above and the index below in the middle). In this way, the Ricci tensor can be thought of as a contraction of the Riemann tensor from the $4 \times 4 \times 4 \times 4$ elements of the Riemann tensor to the 4×4 of the Ricci tensor. The Ricci tensor is a $(0, 2)$-tensor, a function that takes two vectors and gives a scalar as a result.

  In particular, the physical interpretation of the Ricci tensor can be seen by calculating it on two identical vectors: $R(\vec{V}, \vec{V})$ is the proportionality constant that relates volumes and their second derivative rate of change in the direction $\vec{V}$. While the Riemann tensor controls a vector along its parallel transport, the Ricci tensor governs the evolution of small volumes parallelly transported along geodetic curves. Ultimately, the Ricci tensor detects changes in areas/volumes.

  If the geodesics converge, areas and volumes become smaller in the direction $\vec{V}$ and it is said that space has positive Ricci curvature in that direction, $R(\vec{V}, \vec{V}) > 0$; if the geodesics diverge, areas and volumes become bigger and space has negative Ricci curvature $R(\vec{V}, \vec{V}) < 0$. Finally, space has $R(\vec{V}, \vec{V}) = 0$ if areas and volumes remain the same. It is important to notice that $R_{\alpha\beta} = 0$ does not mean the space is flat, but just that space does not cause changes in areas and volumes along geodesics.

- Ricci scalar (R): Ricci scalar is the contraction of the Ricci tensor with the spacetime metric and it is a curvature invariant of a Riemannian manifold that gives global curvature: $R = g^{\mu\nu} R_{\mu\nu}$ or $R = g^{\mu\nu} g^{\rho\tau} R_{\rho\mu\tau\nu}$. It is a $(0, 0)$-tensor, so a function that associates to every point of the Riemannian manifold a real number that is determined by the intrinsic geometry of the manifold . This number characterizes the overall geometry of spacetime, measuring how volumes and areas are distorted: if space has $R > 0$ (positive curvature), the area of a circle of the same radius is smaller than the one in a Euclidean space, else $R > 0$ (negative curvature) means the area of a circle of same radius in that space is bigger than the one in a Euclidean space. Finally, if $R = 0$ the space is flat.

In GR, the metric $g_{\mu\nu}$ in a 4D Lorentzian manifold (the spacetime) is a 4×4 matrix that describes its geometric and causal structure. A metric is a dynamical object, so Einstein's field equations tell how spacetime changes (the independent variables describe time evolution and spatial distribution), given a distribution of mass-energy densities. Namely, Eq. 2.1 is a set of ten-independent[4] second-order differential equations for the metric (both sides are symmetric two-index tensors). However, the Bianchi identity,

[4]The metric tensor $g_{\mu\nu}$ in 4D has 16 independent component as each index can go from 0 to 3, but since it is symmetric, $g_{\mu\nu} = g_{\nu\mu}$, the independent components are just 10.

which is a property of the Einstein tensor (and assures the conservation of the energy-momentum tensor)

$$\nabla^{\mu} G_{\mu\nu} = 0 \ , \tag{2.5}$$

(with $G_{\mu\nu}$ being the Einstein Tensor) reduced them to only six independent equations, as the expression above encloses four constraints. In Einstein's field Eqs. 2.1, one can think of the left-hand side as the geometrical description of spacetime and the right-hand side as the content of matter and energy. It is also important to underline that the Newtonian limit is restored under the following conditions:

- Particles are moving slowly with respect to the speed of light;
- The gravitational field is weak and can be considered as a perturbation of flat space;
- The gravitational field is static.

Einstein's field equations are also non-linear. Therefore, it is very difficult to find a solution: exact solutions can be found only under assumptions such as symmetries and matter content that simplify the problem. For example, Schwarzschild found the solution that bears his name in the vacuum ($T_{\mu\nu} = 0$) assuming spherical symmetry and static (see Sec. 2.1.1).

Once the components of the metric tensor are found, and so how the spacetime's curvature is, it is possible to obtain the trajectories followed by massive particles or light. Indeed the geodesic equation is

$$\frac{d^2 x^{\mu}}{d\lambda^2} + \Gamma^{\mu}_{\nu\alpha} \frac{dx^{\nu}}{d\lambda} \frac{dx^{\alpha}}{d\lambda} = 0 \ , \tag{2.6}$$

where λ can be considered as the proper time for the massive particle or as a generic affine parameter for light. In this case, geodesics represent paths on 4D spacetime followed by a particle that is subjected only to gravity and so generalize the concept of a "straight line" of flat spacetime to a generic manifold (curved manifold). Indeed geodesics are defined as the shortest distance possible between two points on a Riemannian manifold. The geodesic equation is of second-order, as Newton's law of mechanics, and the affine connection can be seen as the "force" that acts on the object (gravity).

David Hilbert was the first to realize that it was possible to derive Einstein's field equations through the principle of least action. This principle is widely used in physics, from classical to quantum mechanics, and also in GR. It states that a physical system follows the path between two states for which the action is minimized. Indeed the action is defined as the integral of the Lagrangian between two states, where the Lagrangian represents an energy function that encloses the dynamics of the physical system. In such a way, the action is a functional that takes the behaviour of a system and returns a scalar. The idea is that since objects that travel in spacetime follow geodesics, the

principle of least action should describe the evolution of a system in a given spacetime. The Einstein-Hilbert action of spacetime is the following,

$$\mathcal{S} = \int dx^4 \sqrt{-g} \left[\frac{1}{16\pi G_N} R + \mathcal{L}_M \right] \ , \tag{2.7}$$

in which $\mathcal{L}_M$ is the contribution from mass densities and g indicates the determinant of the metric. To minimize the action, the variation with respect to the inverse metric must be zero:

$$\begin{aligned} \delta\mathcal{S} &= \int dx^4 \left[\frac{c^4}{16\pi G_N} \frac{\delta(\sqrt{-g}R)}{\delta g^{\mu\nu}} + \frac{R}{\sqrt{-g}} \frac{\delta(\sqrt{-g}\mathcal{L}_M)}{\delta g^{\mu\nu}} \right] \delta g^{\mu\nu} \\ &= \int dx^4 \sqrt{-g} \left[\frac{c^4}{16\pi G_N} \left(\frac{\delta R}{\delta g^{\mu\nu}} + \frac{R}{\sqrt{-g}} \frac{\delta\sqrt{-g}}{\delta g^{\mu\nu}} \right) + \frac{1}{\sqrt{-g}} \frac{\delta(\sqrt{g}\mathcal{L}_M)}{\delta g^{\mu\nu}} \right] \delta g^{\mu\nu} = 0 \ . \end{aligned} \tag{2.8}$$

Since the equation above should be true for all variations $\delta g^{\mu\nu}$, this implies

$$\frac{\delta R}{\delta g^{\mu\nu}} + \frac{R}{\sqrt{-g}} \frac{\delta\sqrt{-g}}{\delta g^{\mu\nu}} = -\frac{16\pi G_N}{c^4} \frac{1}{\sqrt{-g}} \frac{\delta(\sqrt{-g}\mathcal{L}_M)}{\delta g^{\mu\nu}} \ . \tag{2.9}$$

The right-hand side is defined as proportional to the stress-energy tensor

$$T_{\mu\nu} = -2\frac{1}{\sqrt{-g}} \frac{\delta(\sqrt{-g}\mathcal{L}_M)}{\delta g^{\mu\nu}} = -2\frac{\mathcal{L}_M}{\delta g^{\mu\nu}} + g_{\mu\nu}\mathcal{L}_M \ . \tag{2.10}$$

To calculate the left-hand side, it is needed the variation of the Ricci scalar and the determinant of the metric. For this to work, the variation in the Riemann curvature tensor, $\partial R^\rho_{\sigma\mu\nu}$, is first calculated, and then it is contracted. From the expression of the Riemann tensor in Eq. 2.3, its variation can be obtained using the product rule and linearity of derivatives:

$$\delta R^\rho_{\sigma\mu\nu} = \partial_\mu \delta\Gamma^\rho_{\nu\sigma} - \partial_\nu \delta\Gamma^\rho_{\mu\sigma} + \delta\Gamma^\rho_{\mu\lambda}\Gamma^\lambda_{\nu\sigma} + \Gamma^\rho_{\mu\lambda}\delta\Gamma^\lambda_{\nu\sigma} - \delta\Gamma^\rho_{\nu\lambda}\Gamma^\lambda_{\mu\sigma} - \Gamma^\rho_{\nu\lambda}\delta\Gamma^\lambda_{\mu\sigma} \ , \tag{2.11}$$

where $\delta\Gamma^\rho_{\nu\mu}$ is the difference of two Christoffel symbols. Even if the Christoffel symbols (see Eq. 2.4) are not tensor, the variation $\delta\Gamma^\rho_{\nu\mu}$ is a tensor. Indeed the extra derivative term in the transformation of $\Gamma^\rho_{\mu\nu}$, which is independent of the metric, cancels out when evaluating the difference of two Christoffel symbols with $g_{\mu\nu}$ and $g_{\mu\nu} + \delta g_{\mu\nu}$. Therefore, its covariant derivative is:

$$\nabla_\lambda(\delta\Gamma^\rho_{\nu\mu}) = \partial_\lambda \delta\Gamma^\rho_{\nu\mu} + \Gamma^\rho_{\sigma\lambda}\delta\Gamma^\sigma_{\nu\mu} - \Gamma^\sigma_{\nu\lambda}\delta\Gamma^\rho_{\sigma\mu} - \Gamma^\sigma_{\mu\lambda}\delta\Gamma^\rho_{\nu\sigma} \ . \tag{2.12}$$

The variation of the Riemann curvature tensor becomes

$$\delta R^\rho_{\sigma\mu\nu} = \nabla_\mu(\delta\Gamma^\rho_{\nu\mu}) - \nabla_\nu(\delta\Gamma^\rho_{\mu\sigma}) \ . \tag{2.13}$$

Its contraction leads to:

$$\delta R_{\mu\nu} \equiv \delta R^{\rho}_{\mu\rho\nu} = \nabla_{\rho}(\delta\Gamma^{\rho}_{\nu\mu}) - \nabla_{\nu}(\delta\Gamma^{\rho}_{\rho\mu}) \ . \tag{2.14}$$

This expression can then be used to find the variation of the Ricci scalar,

$$\delta R = R_{\mu\nu}\delta g^{\mu\nu} + g^{\mu\nu}\delta R_{\mu\nu} = R_{\mu\nu}\delta g^{\mu\nu} + \nabla_{\sigma}(g^{\mu\nu}\delta\Gamma^{\rho}_{\nu\mu} - g^{\mu\sigma}\delta\Gamma^{\rho}_{\rho\mu}) \ , \tag{2.15}$$

having

$$\nabla_{\sigma} g^{\mu\nu} = 0 \ . \tag{2.16}$$

Since $\sqrt{-g}\nabla_{\sigma}(g^{\mu\nu}\delta\Gamma^{\delta}_{\nu\mu} - g^{\mu\sigma}\delta\Gamma^{\rho}_{\rho\mu})$ is a total derivative, it does not contribute to the action. Indeed, according to the divergence theorem, this term yields a boundary term when integrated, and since the variation of the metric $\delta g^{\nu\mu}$ vanishes at the boundary, it disappears. Thus, we can derive:

$$\frac{\delta R}{\delta g^{\mu\nu}} = R_{\mu\nu} \ . \tag{2.17}$$

Jacob's formula can be exploited to determine the variation of the determinant,

$$\delta_g = \delta \mathrm{Det}(g_{\mu\nu}) = g g^{\mu\nu}\delta g_{\mu\nu} \ . \tag{2.18}$$

In this case, it becomes

$$\delta\sqrt{-g} = -\frac{1}{2\sqrt{-g}}\delta g = \frac{1}{2}\sqrt{-g}(g^{\mu\nu}\delta g_{\mu\nu}) = -\frac{1}{2}\sqrt{-g}(g_{\mu\nu}\delta g^{\mu\nu}) \ , \tag{2.19}$$

having

$$g_{\mu\nu}\delta g^{\mu\nu} = -g^{\mu\nu}\delta g_{\mu\nu} \ . \tag{2.20}$$

The final result for the variation of the determinant of the metric is:

$$\frac{1}{\sqrt{-g}}\frac{\delta\sqrt{-g}}{\delta g^{\mu\nu}} = -\frac{1}{2}g_{\mu\nu} \ . \tag{2.21}$$

Putting together all the terms

$$\frac{\delta R}{\delta g^{\mu\nu}} + \frac{R}{\sqrt{-g}}\frac{\delta\sqrt{-g}}{\delta g^{\mu\nu}} = -\frac{16\pi G_N}{c^4}\frac{1}{\sqrt{-g}}\frac{\delta(\sqrt{-g}\mathcal{L}_{\mathcal{M}})}{\delta g^{\mu\nu}} \ , \tag{2.22}$$

gives finally

$$R_{\mu\nu} - \frac{1}{2}R g_{\mu\nu} = \frac{8\pi G_N}{c^4}T_{\mu\nu} \ . \tag{2.23}$$

When the cosmological constant Λ is included, the action becomes

$$\mathcal{S} = \int dx^4\sqrt{-g}\left[\frac{c^4}{16\pi G_N}(R - 2\Lambda) + \mathcal{L}_{\mathcal{M}}\right] \ . \tag{2.24}$$

Taking the variation of the action with respect to the inverse metric as before and using the least action principle

$$\delta\mathcal{S} = \int dx^4 \left[\frac{\sqrt{-g}}{2K}\frac{\delta R}{\delta g^{\mu\nu}} + \frac{R}{2K}\frac{\delta\sqrt{-g}}{\delta g^{\mu\nu}} - \frac{\Lambda}{K}\frac{\delta\sqrt{-g}}{\delta g^{\mu\nu}} + \sqrt{-g}\frac{\delta\mathcal{L}_M}{\delta g^{\mu\nu}} + \mathcal{L}_M\frac{\delta\sqrt{-g}}{\delta g^{\mu\nu}} \right] \delta g^{\mu\nu} = 0 \ , \tag{2.25}$$

$$\frac{1}{2K}\frac{\delta R}{\delta g^{\mu\nu}} + \frac{R}{2K}\frac{1}{\sqrt{-g}}\frac{\delta\sqrt{-g}}{\delta g^{\mu\nu}} - \frac{\Lambda}{K}\frac{1}{\sqrt{-g}}\frac{\delta\sqrt{-g}}{\delta g^{\mu\nu}} + \frac{\delta\mathcal{L}_{\mathcal{M}}}{\delta g^{\mu\nu}} + \frac{\mathbf{L_M}}{\sqrt{-g}}\frac{\delta\sqrt{-g}}{\delta g^{\mu\nu}} = 0 \ , \tag{2.26}$$

where it has been used $K = \frac{8\pi G_N}{c^4}$ to simplify the notation. Using Eq. 2.17, 2.21 and 2.10 found before

$$\frac{1}{2K}R_{\mu\nu} + \frac{R}{2K}\frac{-g_{\mu\nu}}{2} + \frac{\Lambda}{K}\frac{-g_{\mu\nu}}{2} + (\frac{\delta\mathcal{L}_M}{\delta g^{\mu\nu}} + \mathcal{L}_M\frac{-g_{\mu\nu}}{2}) = 0 \ , \tag{2.27}$$

$$R_{\mu\nu} - \frac{R}{2}g_{\mu\nu} + \Lambda g_{\mu\nu} + K(2\frac{\delta\mathcal{L}_M}{\delta g^{\mu\nu}} - \mathcal{L}_M g_{\mu\nu}) = 0 \ , \tag{2.28}$$

$$R_{\mu\nu} - \frac{R}{2}g_{\mu\nu} + \Lambda g_{\mu\nu} - \frac{8\pi G_N}{c^4}T_{\mu\nu} = 0 \ . \tag{2.29}$$

To summarize what is the conceptual core of GR, gravity has gained a geometrical interpretation in terms of the spacetime curvature (which is flat in SR); energy, in all its variants, determines the curvature of spacetime, which in turn modifies the motion of particles. Einstein's equations of motion and the geodesic equation, which dictates how particles move through spacetime, form instead the core of the mathematical formulation of GR: the solution of Einstein's field equations describes how spacetime is curved by the energy content, allowing us to calculate how particles move across space and time.

2.1 Black Holes

In the 18^{th} century, Michell [67] and Laplace [57] introduced the concept of "dark star", making use of Newton's gravitational laws and the corpuscular theory of light. According to them, these objects would be so massive and compact that the escape velocity would have to be greater than the light speed, making them dark.

With the advent of GR,"dark stars" have been seen in a new "light", and their description has evolved into what is now known as BHs. BHs are predicted by GR, but since their formulation, these solutions have raised perplexity due to the enigmatic phenomena they imply. They are defined as the region of spacetime characterized by the presence of the event horizon, a boundary of spacetime that separates events that can communicate with distant observers from those that cannot (see Fig. 2.3).

This means that everything that crosses the event horizon will never again be able to reverse its course and that everything within it is trapped and can never reach outside

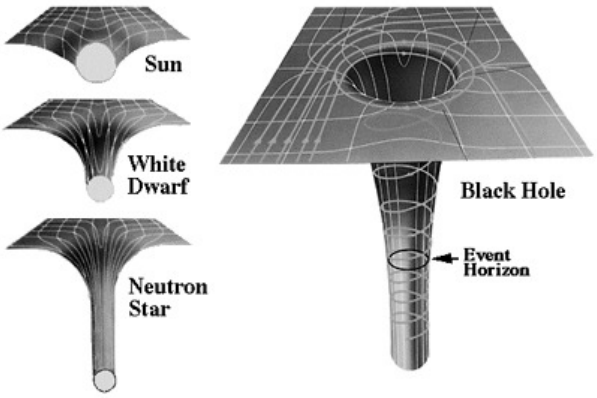

Figure 2.3: For a BH to exist there is no necessity for a singularity as long as a horizon is formed. The BH is the horizon.

observers. For this reason, the term BH refers to the event horizon: not even light can leave this boundary and reach us as distant observers. The formation of such a horizon follows from the collapse of matter in a region where the curvature, and therefore the gravity, is so intense (tending to infinity in the singularity) to trap even the light.

Another important aspect that characterizes BHs in the framework of GR is the no-hair theorem. The no-hair theorem asserts that all stationary BH solutions of the Einstein-Maxwell field equations are completely identified by their mass, electric charge, and angular momentum. This means that if any two BHs share the same value for these parameters, then they are indistinguishable. Its importance lies in the fact that it provides a framework where to test GR. The aim is to use advanced tools and techniques to measure with high precision properties of BHs, searching for possible violations of this theorem. This is made more difficult by the fact that, due to their nature, BHs can not be directly detected, but for example, a BH presence can be inferred through its gravitational effects on the surrounding or through gravitational waves produced during their merges. BH studies are still far from a complete understanding of these exotic objects. One approach to address this is by formulating different BH models with various types of gravity. Indeed, they provide the perfect natural 'laboratory' for studying gravity in the strong-field regime. BHs in modified gravity theories are thought to affect the large-scale structure and the overall dynamics of the Universe. It remains an open question whether we can detect deviations from GR under the influence of a scalar field in BH thermodynamics (properties such as entropy and temperature), BH shadows, or gravitational wave signals from their mergers.

2.1.1 Schwarzschild solution

In 1916 Karl Schwarzschild found what can be considered as the simplest BH solution. The Schwarzschild metric is indeed a solution to the Einstein equation in the vacuum ($T_{\mu\nu} = 0$[5]), which describes spacetime around a spherically symmetric mass:

$$ds^2 = -\left(1 - \frac{2G_N M}{r}\right) dt^2 + \frac{dr^2}{1 - \frac{2G_N M}{r}} + r^2\left(d\theta^2 + \sin^2\theta d\phi^2\right) , \tag{2.30}$$

having $c = 1$, where $\{t, r, \theta, \phi\}$ are the Schwarzschild coordinates, adapted to the spherical symmetry of spacetime (in particular r is the areal radius), G_N is the Newton's constant and M the Newtonian mass. Associated with this solution, there is a characteristic length scale, the Schwarzschild radius, that defines the size of the event horizon:

$$R_H = \frac{2G_N M}{c^2} = 2G_N M \ . \tag{2.31}$$

Moreover, this solution is characterized by asymptotic flatness: when $r \gg 2G_N M$ Minkowski flat metric is restored. The closer you get to R_H, the more these observers deviate from being inertial observers. As the Birkhoff theorem demonstrates, the Schwarzschild solution is also the unique and more general possible with the conditions above. Therefore, it defines the spacetime outside every non-rotating spherical symmetrical source without charge. When being sufficiently distant, there is no observational difference between the gravitational field caused by a BH or any other spherical source (for example, a star or a planet) with the same mass. However, some peculiar phenomena occur when it is possible to approach the Schwarzschild radius R_H. This is the case only for BHs, extremely dense and compact objects that are entirely contained within R_H. As it can be noticed by Eq. 2.30, the metric has two singularities at $r = R_H$ and $r = 0$ (see Fig. 2.4).

The first one is a coordinate singularity and can be removed by a coordinate transformation. One way to verify that R_H is not a special region for spacetime is to calculate the curvature scalars[6] (quantities that are independent of the choice of coordinates). The easiest one would be the Ricci scalar R, but in this case (asymptotically flat spacetime) it is necessarily null, and the same is for the contraction of the Riemann Tensor with itself, $R_{\mu\nu}R^{\mu\nu}$. What can be used is instead the Kretschmann scalar (local curvature) for the Schwarzschild solution:

$$R^{\mu\nu\rho\sigma}R_{\mu\nu\rho\sigma} = \frac{48G_N^2 M^2}{r^6} \ , \tag{2.32}$$

that calculated in R_H does not diverge. Moreover, when considering radially infalling geodesics, they can cross R_H without problems: a particle which falls radially reaches and

[5] Taking the trace of Einstein's tensor (with $\Lambda = 0$.) we get $R = 0$. In this way the Einstein vacuum equations simplify to $R_{\mu\nu} = 0$.

[6] All curvature scalars can be built from the Riemann Tensor.

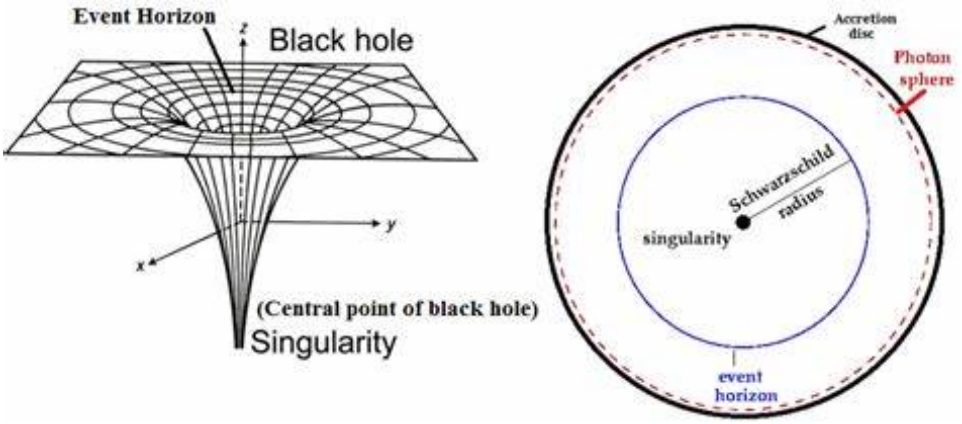

Figure 2.4: In the image it is represented not only the coordinate singularity (event horizon) and the physical singularity at the center but also the photon sphere and the accretion disk. The photon sphere is a boundary where photons are trapped in circular unstable orbits. The accretion disk is formed by diffuse material (gas and dust) orbiting around the BH, spiraling inward, and heated by friction. This is the cause of electromagnetic radiation, often in the X-ray.

crosses the Schwarzschild radius in a finite proper-time, while the fact that the coordinate time diverges is another symptom of the fact that the Schwarzschild coordinates are not suitable for describing the totality of the trajectory. Lastly, it is possible to estimate the radial tidal force from the components of the Riemann tensor:

$$\frac{\delta \ddot{r}}{\delta r} \simeq \frac{G_N M}{r^3} \ , \tag{2.33}$$

and see that they have a finite value in R_H. All these considerations lead to the conclusion that R_H is not a boundary between two distinct manifolds, but rather the Schwarzschild manifold is unique and requires at least two charts[7] to be covered.

Completely different is instead the singularity at $r = 0$, as it is a true physical singularity, where the curvature of spacetime becomes infinite and spacetime itself breaks down. There, invariant curvature scalars become infinite, and geodesics are incomplete. At that point, even the radial tidal forces diverge. Thus, $r = 0$ is the gravitational singularity at the center of BH, enclosed by the event horizon at the distance R_H, just a coordinate singularity. This latter is a boundary in spacetime but, at least locally, it does not show any peculiarity: in case an astronaut happens to survive crossing the horizon of Schwarzschild, he cannot notice anything strange or different (the components of the Riemann tensor in a local inertial system are also finite in $r = R_H$); however, the

[7] A chart is defined as the set (A, ψ), being A a subset of the manifold $\mathcal{M}$ ($A \subseteq M$) and ψ an invertible continuous map $\psi : A \to \mathbb{R}^n$.

Schwarzschild horizon is a causal horizon, and the astronaut cannot reverse course. Indeed, using the Schwarzschild coordinates t, r, θ, ϕ in the domain $r > R_H$, the metric has signature $-,+,+,+$, while in the domain $r < R_H$ the signature is $+,-,+,+$. Furthermore, for $r \to R_H^+$, $\quad g_{tt} \to 0$ e $g_{rr} \to +\infty$ while for $r \to R_H^-$, $\quad g_{tt} \to 0$ e $g_{rr} \to -\infty$[8]. This demonstrates that g_{tt} and g_{rr} change sign across R_H and, for $r < R_H$, t is a spatial coordinate and r become a time-like coordinate. Since particles must follow a time-like trajectory, once they have crossed R_H, they will be forced to follow a trajectory that continuously evolves r, inevitably directed towards $r = 0$ and, therefore, towards the center.

This fate is also common to any photon that is within the Schwarzschild radius: if a particle that has crossed R_H emits a photon, it will also be forced to follow a direct trajectory forward in "time", that is towards decreasing values of the r coordinate. The meaning of all of this is that the singularity $r = 0$ is in the future of any time or light-like trajectory inside R_H, *i.e.* all particles and photons are destined to precipitate inevitably towards the center.

This shows how everything that crosses the Schwarzschild radius remains trapped inside, with no way to get out of it and thus no way to communicate with any observer outside R_H. From it, the definition of the Schwarzschild radius as the Schwarzschild horizon. At the Schwarzschild horizon, distant observers experience the effects of gravitational time dilation and gravitational redshift, as predicted by Einstein. The first one comes from the fact that, as it has already been said, the time component of the Schwarzschild solution diverges when approaching R_H. From the viewpoint of an asymptotically inertial observer placed at $r \gg R_H$, the time component is their proper time. Therefore, the particle takes an infinite amount of time to reach the Schwarzschild radius, and in fact, he would never see it cross it. In other words, clocks near a BH would appear to tick slower than those farther away from the BH.

At the same time, if the particle is sending light signals, the gravitational redshift in the Schwarzschild metric is described by the following expression:

$$\omega_n = \omega_s \sqrt{\frac{1 - v_n}{1 + v_n}} \sqrt{1 - \frac{R_H}{r_n}} \ , \tag{2.34}$$

where ω_n is the frequency of the n-th emission that an asymptotically inertial observer receives. The first square root is the contribution from the Doppler effect for a particle falling with velocity v_n, and the second square root represents the gravitational redshift effect (see Fig. 2.5). As a consequence, asymptotically inertial observers receive fainter light signals at increasing intervals until $r \to R_H$, where their intensity decreases to zero (the energy of the emitted photon is redshifted) and the receive interval tends to infinity (the particle appears to freeze at the event horizon). Hence, we would observe a particle that slows down more and more as it gets closer to the Schwarzschild radius, and that

[8]This is indeed what defines a horizon: the $g_r r$ component of the metric diverges.

sends light signals tending more and more toward the red wavelengths until the photon that starts from the Schwarzschild radius spends all its energy before it can be detected by us (it is said to undergo an infinite gravitational redshift, its frequency approaches zero). Eventually, the falling object fades away until it can no longer be seen and we would never see the particle actually reaching and crossing R_H.

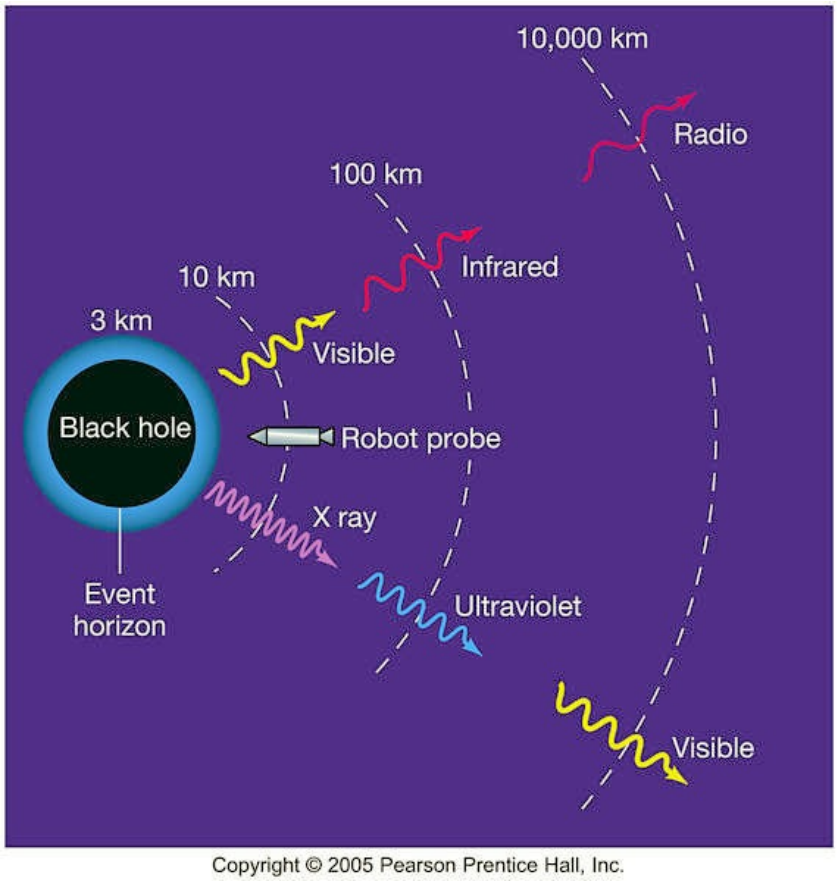

Figure 2.5: Imaging a probe that is radially falling towards a BH and is emitting light signals, their wavelength will be stretched due to the gravitational redshift effect.

2.1.2 Reissner-Nosträm solution

Schwarzschild's BHs refer to the simplest type, of spherical symmetry, with just mass and without any electric charge or angular momentum. But this is not the only one. There exist also solutions that describe more general BHs. Non-rotating and spherically symmetric BHs with an electric charge are described by the Reissner-Nosträm (RN) metric, a static and stationary solution to the Einstein-Maxwell field equations.

In Schwarzschild-like coordinates t, r, θ, ϕ:

$$ds^2 = -\left(1 - \frac{R_H}{r} + \frac{R_Q^2}{r^2}\right) dt^2 + \frac{dr^2}{1 - \frac{R_H}{r} + \frac{R_Q^2}{r^2}} + r^2\left(d\theta^2 + \sin^2\theta d\phi^2\right) , \tag{2.35}$$

where R_H is defined as in Eq. 2.31, while R_Q is the characteristic length scale corresponding to an electric charge Q given by:

$$R_Q^2 = \frac{Q^2 G_N}{4\pi\varepsilon_0 c^4} , \tag{2.36}$$

with ε_0 the electric permissivity in the vacuum. In particular, RN BHs have two concentric event horizons (see Fig. 2.6), identified by the following equation[9]:

$$r_\pm = \frac{1}{2}\left(R_H \pm \sqrt{R_H^2 - 4R_Q^2}\right) . \tag{2.37}$$

These two event horizons become degenerate for $2R_Q = R_H$, indicating an extremal BH. It can not exist a BH with $2R_Q > R_H$ as if the charge is greater than the mass, then the term under the square root becomes negative and no physical horizons could exist.

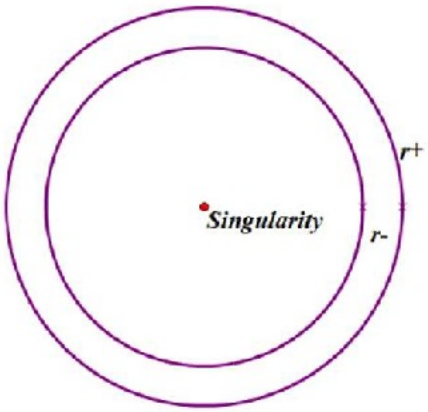

Figure 2.6: In the image there are represented the two horizons that characterized a non-rotating and spherically symmetric BH

2.1.3 Kerr-Newmann solution

Finally, the most general known solution for a BH, which has both angular momentum and charge is the Kerr-Neumann BH (see Fig. 2.7). Indeed, the Kerr-Neumann metric is

[9]The radius at which the component g_{rr} diverges defines the horizons.

a vacuum solution of the Einstein-Maxwell field equations that describes the spacetime geometry around a mass that is electrically charged and rotating. In the Boyer-Lindquist coordinates:

$$ds^2 = -\left(\frac{dr^2}{\Delta} + d\theta^2\right)\rho^2 + (cdt - a\sin^2\theta d\phi)^2\frac{\Delta}{\rho^2} - ((r^2+a^2)d\phi - acdt)^2\frac{\sin^2\theta}{\rho^2}\ , \quad (2.38)$$

where R_H is defined as in Eq. 2.31, R_Q as in Eq. 2.36, and

$$a = \frac{J}{Mc}, \quad \rho^2 = r^2 + a^2\cos^2\theta, \quad \Delta = r^2 - R_H r + a^2 + R_Q^2\ . \quad (2.39)$$

Even if the mass M of a BH can take any positive value, its total electric charge Q and angular momentum J are constrained by the mass following the condition below:

$$\frac{Q^2}{4\pi\varepsilon_0} + \frac{c^2J^2}{G_N M} \leqslant G_N M^2\ . \quad (2.40)$$

For a non-rotating BH, the singularity takes the shape of a single point, while for a rotating BH, it is smeared out to form a ring singularity that lies in the plane of rotation. In both cases, the singular region has zero volume, contains all the mass of the BH, and therefore has infinite density.

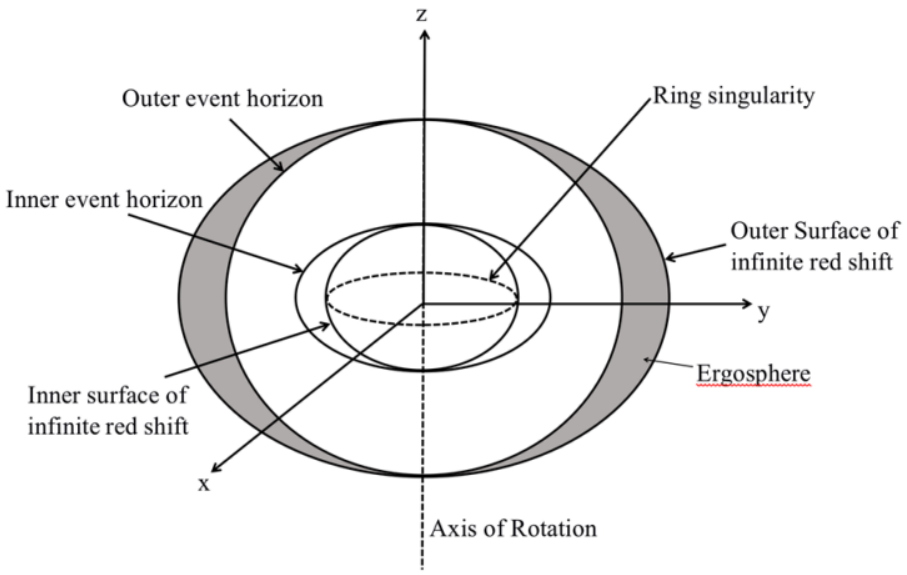

Figure 2.7: The picture shows schematically the structure of a Kerr-Newmann BH. In particular, it presents the ergosphere, a region of spacetime that surrounds rotating BHs, due to frame-dragging. It can be noticed that it coincides with the event horizon at the poles while it enlarges on the equatorial plane. Inside the ergosphere, an object cannot stand still, but it moves in the direction of the BH rotation. Indeed, that object would have to move faster than the speed of light in the opposite direction to just stand still. In the image, it can also be noticed the ring singularity.

Chapter 3

Beyond GR

In the introduction, some of the mysteries and questions that modern physics is struggling with were presented. In particular, GR does not fully describe DM and DE on a large cosmological scale since it predicts their effects but does not go inside their fundamental nature. For this reason, the idea that corrections are needed in order to have a complete theory of gravity that is able to explain all the observable universe is of growing interest [71, 24, 72]. As GR correctly describes the gravitational interaction in high curvature and reduces to Newton's theory of gravity - which has been verified to correctly describe interactions in low curvature and small scales - the future perspective is to extend GR in those regimes where nowadays it seems to fail. This section aim is to present some of the paths that researchers are following to build a consistent theory of gravity and discover the true nature of our Universe.

There exist two fundamental theorems that guide the development of the gravitational action for other possible theories: Lovelock's theorem [59] and Ostrogradky's theorem [69, 92]. While the former states the uniqueness of GR under precise conditions, thus laying the foundations for finding alternative ways beyond GR, the latter restricts the equations of motion (EOM) to be at most second-order in order to avoid runaway negative energy.

3.1 Lovelock's theorem

Lovelock's theorem (1971) states that, in 4D, the only second-order Euler-Lagrange equations for a metric which are derivable from an action that contains only the 4D metric and its derivatives up to the second-order are the Einstein's field equations. In other words, Lovelock assures that GR *is the only gravity theory in* $4D$ that satisfies the following assumptions:

- Second-order equation of motion for the metric;

- Spacetime is 4D;
- Locality;
- No extra fields, which means that only the metric is involved in the gravitational action, and there are no extra degrees of freedom;
- Covariance, meaning that laws of physics are invariant under arbitrary differentiable coordinate transformations.

Therefore, to go beyond GR and elaborate alternative gravity models, one must abandon some of these assumptions. Since any gravitational theory other than GR can be thought of as a possible way around Lovelock's theorem, it is evident how modifications of GR separate in many different branches. Examples of these are:

- Beyond second order EOM;
- Higher dimensional spacetime;
- Non-local theories;
- Add new field content and extra degrees of freedom (scalar, vector, tensor).

Every proposed model takes into consideration one or more of these possible modifications to GR. By changing the nature of the constraints of the theory, it ends up freeing new degrees of freedom.

Lovelock also expanded his thoughts on higher dimensions, elaborating the most general metric theory of gravity in N-dimensions (ND hereafter) that satisfy the following conditions:

- Symmetric;
- Divergence-free;
- Depends on metric and its derivatives up to the second-order.

He studied what could be, in any given ND, the most general combinations of geometric invariants that one can add in the action, such as it yields to second-order EOM. The resulting unique ND theory of gravity, which has the same properties as GR, contains non-linear corrections to the Einstein-Hilbert Lagrangian. These corrections account for the additional dimensions and ensure that the theory reduces to Einstein's GR in 4D spacetime. As it can be seen in Tab. 3.1, these corrections are different ways of contracting the Riemann tensor, while in 4D, the only independent scalar constructed out of the Riemann tensor, $R_{\mu\nu\sigma\rho}$, that will give EOM that are not higher than second-order for the metric, is the Ricci scalar R. These additional terms are known as Lovelock invariants: they generalized the Eintein-Hilbert action of GR, and led to modified field equations.

Table 3.1: Unique gravity Lagrangians in higher dimensional spacetimes

Spacetime	Unique gravity Lagrangian
D=3, 4	$L_I = R + \Lambda$
D=5, 6	$L_{II} = L_I + \alpha_{GB} L_{GB}$ $L_{GB} = R_{\alpha\beta\gamma\delta} R^{\alpha\beta\gamma\delta} - 4R_{\alpha\beta} R^{\alpha\beta} + R^2$
D=7, 8	$L_{III} = L_{II} + R^3 + 3RR^{\mu\nu\alpha\beta} R_{\alpha\beta\mu\nu} - 12RR^{\mu\nu} R_{\mu\nu} + 24R^{\mu\nu\alpha\beta} R_{\alpha\mu} R_{\beta\nu}$ $+16R^{\mu\nu} R_{\nu\alpha} R^{\alpha}_{\mu} + 24R^{\mu\nu\alpha\beta} R_{\alpha\beta\nu\rho} R^{\rho}_{\mu} + 8R^{\mu\nu}{}_{\alpha\rho} R^{\alpha\beta}_{\nu\sigma} R^{\rho\sigma}_{\mu\beta} + 2R_{\alpha\beta\rho\sigma} R^{\mu\nu\alpha\beta} R^{\rho\sigma}{}_{\mu\nu}$

Thus, Lovelock's work has led to the natural generalization of Einstein's GR to higher dimensions. Lovelock's gravity indicates the most general metric theory of gravity in ND spacetime yielding second-order EOM. The formulation of the Lovelock's gravity in ND is the following:

$$\mathcal{L} = \sqrt{-g} \sum_{n=0}^{n=j} \alpha_n \mathcal{R}^n, \quad \mathcal{R}^n = \frac{1}{2^n} \delta^{\mu_1,\nu_1 \cdot \mu_n \nu_n}_{\alpha_1 \beta_1 \cdot \alpha_n \beta_n} \prod_{i=1}^{n} R^{\alpha_i \beta_i}{}_{\mu_i \nu_i} \ , \tag{3.1}$$

where

$$\delta^{\mu_1,\nu_1 \cdot \mu_n \nu_n}_{\alpha_1 \beta_1 \cdot \alpha_n \beta_n} (2n)! \delta^{\mu_1}_{[\alpha_1} \delta^{\nu_1}_{\beta_1} \cdot \delta^{\mu_n}_{\alpha_n} \delta^{\nu_n}_{\beta_n]} \ , \tag{3.2}$$

is the generalized Kronecker delta (anti-symmetric product of Kronecker deltas), $R^{\alpha_i \beta_i}{}_{\mu_i \nu_i}$ is the Riemann tensor, and j is such that $D = 2j+2$ for even dimensions and $D = 2j+1$ for odd dimensions. The action in higher dimensions is thus given by Euler densities which are polynomials in the Riemann tensor (Lovelock invariants) and give second-order EOM.

3.2 Ostrogradsky's theorem

Ostrogradsky's theorem establishes the importance of having EOM at most of the second-order. Indeed, he showed that, otherwise, non-degenerate Lagrangians with time-derivatives higher than the first lead to Hamiltonians that are unbounded from below. These dynamical systems can not be physical, leading to Ostrogradksy instabilities: the energy of the system can have any arbitrarily negative value. Ostrogradsky's theorem can be seen as an explanation for why physical phenomena are all described by differential equations of second-order (Newton's equations of motion, Maxwell's equations, Einstein's equations...). For example, it can be considered a Lagrangian which depends on $q(t)$, the generalized coordinates of the system (for example, θ for a simple pendulum), and its

first (generalized velocities) and second time-derivatives:

$$L \equiv L(q, \dot{q}, \ddot{q}) \ . \tag{3.3}$$

The Euler-Lagrange equation is

$$\frac{\partial L}{\partial q} - \frac{d}{dt}\frac{\partial L}{\partial \dot{q}} - \frac{d^2}{dt^2}\frac{\partial L}{\partial \ddot{q}} = 0 \ . \tag{3.4}$$

Assuming non-degeneracy, $\frac{\partial^2 L}{\partial \ddot{q}^2} \neq 0$, then

$$q^{(4)} = F(q, \dot{q}, \ddot{q}, q^{(3)}) \quad \rightarrow \quad q = G(t, q_0, \dot{q}_0, \ddot{q}_0, q_0^{(3)}) \ . \tag{3.5}$$

The equations of motion are of fourth-order, and since the solution depends on four initial conditions, there must be four canonical coordinates. In particular, non-degeneracy implies that the phase space transformation can be inverted, and the canonical coordinates can be expressed in terms of q and vice versa. They are given by:

$$Q_1 \equiv q \ , \quad Q_2 \equiv \dot{q} \ , \quad P_1 \equiv \frac{\partial L}{\partial \dot{q}} - \frac{d}{dt}\frac{\partial L}{\partial \dot{q}} \ , \quad P_2 \equiv \frac{\partial L}{\partial \ddot{q}} \ . \tag{3.6}$$

The Hamiltonian is defined in the standard way as:

$$\begin{aligned} H(X_1, X_2, P_1, P_2) =& P_1\dot{Q}_1 + P_2\dot{Q}_2 - L(Q_1, Q_2, \dot{Q}_2) \\ =& P_1\dot{Q}_1 + P_2 f(Q_1, Q_2, P_2) - L(Q_1, Q_2, f(Q_1, Q_2, P_2)) \ , \end{aligned} \tag{3.7}$$

where (due to nondegeneracy)

$$\dot{Q}_2 = f(Q_1, Q_2, P_2) \ . \tag{3.8}$$

The Hamiltonian is linear in the canonical momentum variable P_1, it is unbounded from below, and hence the system can not be stable as it could have a negative energy value (Ostrogradsky instability). Thus, when building new scalar-tensor theories, the requirement of EOM of second-order is one of the most important constrain to impose in order to have a theory of gravity free from Ostrogradsky instability.

3.3 Scalar Fields

As has already been mentioned in the previous section, one possible way to overcome Lovelock's theorem, and so GR, is to introduce new degrees of freedom. This can be done, for example, by introducing new scalar, vectorial, or tensorial fundamental fields. In particular, scalar fields are recently being employed in many realms of physics: they appear in unified theories (string theory) and many alternative theories of gravity. They

have been of particular interest because of the new possibility they open to study and interpret the Universe. Some of them are thought to be at the very basics of the Universe [78, 81, 14, 65, 64, 42, 87].

In the Standard Model of particle physics, the Higgs boson was finally detected in 2012 by ATLAS and CMS [27]. This is a massive scalar field with the role of giving mass to elementary particles through the Higgs mechanism.

Scalar fields have been also employed in the development of quantum gravity, in the attempt to unify GR and quantum mechanics [34].

In Cosmology, during the inflationary period, a scalar field is the possible responsible for the non-adiabatic cosmic expansion of the Universe in its early history [94]. Its physical nature is still under debate, but there might be connections with the Higgs boson itself [84], the dilaton field of string theory in the context of quantum gravity [56], or even with the modified theories of gravity [79].

In the framework of gravitation, including scalar fields, either in the matter or in the gravitational sector of the theory, can provide an alternative theory of gravity addressing some of the still open questions. One of the most important is to give an explanation for the late accelerated expansion and to investigate the role and origin of DE. Moreover, it seems from observations that it has to be taken into account also a large quantity of non-baryonic matter, known as DM (see Sec. 1). Again, scalar fields are investigated as possible candidates for both DM and DE [80, 42].

Scalar-tensor theories introduce a scalar field non-minimally coupled with various curvature terms in the Lagrangian. In such a way, the gravitational interaction is affected by the presence of the scalar field and this leads to phenomena that mimic the effect of DE and DM. When building a scalar-tensor model, one must always be subjected to Ostrograsky's theorem (see Sec. 3.2) and ensure that it yields second-order EOM. In particular, this is the case of the extended scalar-tensor theories. While scalar-tensor theories are generally referred to as theories whose Lagrangian contains a scalar field that is non-minimally coupled to the Ricci scalar and possibly its kinetic and potential energy, extended scalar-tensor theories are considered as a generalization since they also include higher-order derivatives of the metric and scalar field.

Containing higher-order derivatives allows for more intricate interactions between the scalar field and the curvature of spacetime, but it can also lead to instabilities due to higher-order EOM (unphysical solutions with negative energy). Indeed, following the principle of least action to obtain the Euler-Lagrange equations, higher-order derivatives in the Lagrangian contribute with additional derivatives in the EOM. This is why such theories should be built with constraints to avoid this kind of instability brought by higher-order derivative terms. Lastly, scalar-tensor theories are also subject to observational constraints, such as local tests of gravity. This means that the effects of such scalar fields should be suppressed at scales where GR is well tested (laboratories on Earth and the Solar System). In this context, the scalarization mechanism is particularly interesting for theories that include scalar fields that are non-minimally coupled to gravity.

According to this mechanism, scalar fields become activated in strong-gravity regimes (high curvature), while their effects are absent in the weak-gravity regime. In this way, it is possible to restore GR.

3.3.1 Scalarization

In the framework of scalar-tensor theories and extended scalar-tensor theories, scalarization would provide a mechanism able to leave scalar imprints detectable by our experiments. Indeed, an intriguing future achievement would be to test GR and BH models through precision astrophysical observations, especially in the field of gravitational waves, and eventually reveal the existence of new fundamental fields [50, 17]. As has already been mentioned (see Sec.3), one of the most immediate ways to modify GR is to introduce a scalar field that is non-minimally coupled to gravity. However, such fields have remained so far undetected. This is why, in general, scalar-tensor theories come with some observational constraints: in the weak gravity regime, GR must be restored since this theory has successfully passed every test in that regime (*e.g.* Earth laboratories, Solar System observations) [26]. Nonetheless, such theories are also characterized by the fact that certain conditions and interactions can lead to a non-trivial configuration for the scalar field thanks to the coupling of the scalar field with matter or curvature of the spacetime. This coupling can cause the scalar field to become significant under specific circumstances, leading to observable effects that differ from those predicted by GR.

Scalarization is a mechanism with many different shades: it can be triggered by a strong coupling between the scalar field and the spacetime curvature (non-vanishing scalar field near compact objects such as BH and Neutron Stars [82]), by changes in the surrounding environment (for example in a binary neutron stars system [74]) or by the increasing coupling between the scalar field and matter fields. In what follows, just the scalarization due to the non-minimal coupling with curvature terms is considered. Moreover, it is possible to distinguish between spontaneous scalarization, simply due to the instabilities of the system that cause the scalar field to grow, and induced scalarization, which is triggered by external factors.

In this case, a strong gravitational field, such as the one near BHs, can act as a trigger for scalarization: in the presence of a region of intense spacetime curvature, the coupling between the scalar field and the spacetime curvature can become so strong that the scalar field is excited, becomes unstable and grows significantly. As a result, BHs could develop a non-trivial scalar configuration, or in other words, "grow hair". Thus, these theories would be able to evade the no-hair conjecture, admitting new branches of solutions with respect to GR. In particular, it has been shown that generalized gravity theories with higher-curvature terms, such as the quadratic Gauss-Bonnet term, non-minimally coupled to the scalar field can evade both the old no-hair conjecture and the novel no-hair conjecture [5, 52]. The first one was conceived in the context of GR and states that every BH can be described by only three external observable properties, mass, electric charge,

and angular momentum [13]. The second one has been developed successively, with the discovery of BHs with Yang-Mills [89] or Skyrme fields, and extends to the introduction of additional fields like scalar fields [61]. Among ESTTs, the coupling function between the GB term and the scalar field plays an important role in the scalarization mechanism since it determines how the scalar field interacts with gravity. When gravity (curvature) exceeds a certain threshold, it activates the scalar field (scalarization is triggered) - while it does not exist in weak gravity - and different types of coupling functions can lead to novel hairy BHs through different types of scalarization under certain conditions.

In the Einstein-dilaton-Gauss-Bonnet theory, the linear or exponential coupling functions $f(\phi) = \alpha\phi$ or $f(\phi) = \frac{1}{\alpha}(1 - e^{\alpha\phi})$ (with α the coupling constant) lead to BHs always surrounded with hairs [53, 55, 85, 54, 55]. In other words, it does not admit Schwarzschild BH solutions, but all static and stationary, spherically symmetric BH solutions in this theory have non-trivial scalar field configurations. Since $\phi(r) = 0$ does not solve the field equations, the condition on the coupling function must be:

$$\frac{df(\phi)}{d\phi}\Big|_{\phi=0} \neq 0 \quad . \tag{3.9}$$

Spontaneous scalarization [36, 82, 5] is instead characterized by couplings such as $f(\phi) = \alpha\phi^2$ and $f(\phi) = \frac{1}{2\alpha}(1 - e^{-\alpha\phi^2})$. It was found that, below a certain critical mass, the Schwarzschild BH becomes linearly unstable as a solution in the ESTGB theory, and new branches of scalarized BH develop [70]. The scalarized branches form a discrete family of solutions labeled by the number of nodes or zeroes of the scalar field profile. The phase transition is triggered in the strong-gravity regime by a tachyonic instability: due to the non-minimal coupling of the scalar field with the spacetime curvature, whenever the gravitational field (and so the spacetime curvature) exceeds some threshold, the scalar field could acquire a sufficiently negative effective mass. This makes the scalar field unstable, and thus it grows under small perturbations. At that point, scalarized solutions are energetically and entropically more stable than the Schwarzschild BHs, and they are so preferred. The effective mass is given by the term

$$\frac{d^2 f(\phi)}{d\phi^2} I \quad , \tag{3.10}$$

obtained from the linearized Klein-Gordon equation, and it must be

$$\frac{df(\phi)}{d\phi}\Big|_{\phi=0} = 0 \quad , \tag{3.11}$$

$$\frac{d^2 f(\phi)}{d\phi^2}\Big|_{\phi=0} \neq 0 \quad , \tag{3.12}$$

which are the conditions for the coupling function to have spontaneous scalarization. The fact that the scalar field exists only in regions of strong curvature of spacetime allows

us to restore GR in the weak field regime, thus satisfying observational constraints. In the case of spontaneous scalarization (ignited by tachyonic instability), both free-scalar solution and scalarized solution can exist as equilibrium solutions and even a small perturbation can lead to the transition from one to the other. The literature of BH spontaneous scalarization has been largely extended: they have also studied rotating BH [30, 46, 47, 33, 16, 29], charged BH [51, 21, 39, 8], spinning and charged BH [45] and spin-induced scalarization (if the dimensionless spin parameter exceeds a critical value, the effective mass squared of the scalar field becomes negative) [37, 4]. In the case of scalarization of asymptotically flat, charged BH (RN BH) in the Einstein-Maxwell-scalar models (EMS)[1], a sufficiently large charge-to-mass ratio makes RN BH unstable under scalar perturbations.

Non-linear scalarization [35] is possible when the coupling functions contain higher and even power of the scalar field: $f(\phi) = \beta\phi^4$ or $f(\phi) = \frac{1}{4\beta}(1 - e^{-\beta\phi^4})$. In this case, Schwarzschild BHs are stable solutions under linear perturbations and at least two types of scalarized Schwarzschild solutions are admissible. This time, the transition is made possible by large non-linear perturbations. The same phenomenon in the context of EMS is described in [18, 19]. This time, the condition on the coupling function should be:

$$\frac{d^2 f(\phi)}{d\phi^2}\Big|_{\phi=0} = 0 \quad . \tag{3.13}$$

Recently, more extensions within the scalarization process have gained interest. For example, it is possible to consider a mixture of linear and non-linear scalarization in order to investigate how the higher-order power of the scalar field affects the properties of the scalarized BHs and their stability [68, 15]. Moreover, the presence of mass or self-interaction terms can quench or suppress scalarization leading to scalarized solutions under different conditions [75].

For future research, it is important to build different models to study scalarization and evolution of the scalar field under various conditions. Through scalarization, ESTTs introduce novel hairy BH solutions with respect to GR (BHs with a non-trivial scalar configuration), and, at least from a theoretical point of view, these would carry distinct and different characteristics. Indeed, the shadow of a BH, as the one detected by the Event Horizon Telescope (EHT) [7], can be influenced by the presence of a scalar field, showing differences in the shape or size as predicted by GR. Furthermore, scalar fields could leave their imprints in gravitational wave signals (for example modifications in the amplitude, phase, and frequency) [50]. In addition to that, it can be considered also deviations in the orbital dynamics around scalarized compact objects [38], accretion disks of BH [22] or pulsar timing [66], or even X-ray and radio emission from neutron stars and BH accretion disks [93]. The hope is in the future to reach sufficient precision in the experimental and observational field to test the theoretical models.

[1]Non-minimal coupling between the scalar field and the Maxwell invariant $F_{\mu\nu}F^{\mu\nu}$.

3.4 Gauss-Bonnet Scalar-Tensor theory

Among ESTTs, this study considers the ESTGB, which includes a scalar field non-minimally coupled with the GB term. This latter is a particular combination of curvature scalars,

$$I = R^2 - 4R_{\mu\nu}R^{\mu\nu} + R_{\mu\nu\rho\delta}R^{\mu\nu\rho\delta} \ , \tag{3.14}$$

which is a property of spacetime and contains corrections to the curvature, similar to a Taylor series. Indeed, it introduces overall second-order correction to the curvature (a combination of the second derivative of the metric).

The GB invariant is composed of three quantities that mathematically describe the curvature of spacetime (of any Riemannian manifold[2]). In particular, it is a quadratic combination of the following curvature tensors: R the Ricci scalar, $R_{\mu\nu}$ the Ricci tensor, and $R_{\mu\nu\rho\delta}$ the Riemann tensor (see Sec. 2). The fact that the GB term contains quadratic combinations of the curvature tensors makes it a higher-order correction compared to the linear Einstein-Hilbert action, which contains only the Ricci scalar.

When the GB is integrated over a 4D spacetime manifold, the result is a constant called the Euler number. This latter is a topological invariant that describes the space's shape and structure. Consequently, when varying the action to obtain the equation of motion (principle of least action), its contribution vanishes. Indeed, in 4D, the GB term is topological, thus its integral reduces to a boundary integral according to the divergence theorem, and this latter identically vanishes. Only in higher dimensions the GB term is non-trivial. However, scalar-tensor theory in 4D manages to make I contribute to gravitational dynamics by multiplying it by a function of the scalar field. In this way, the GB invariant is the unique quadratic curvature combination that still gives second-order equations in the metric (higher orders cancel each other out, and Ostrogradsky's theorem is satisfied). Therefore, the modified gravity with ESTGB arises by combining the GB invariant with the Einstein-Hilbert action; the former represents a higher-order curvature term and introduces corrections to the gravitational field equations, keeping them of second-order in the derivatives of the metric.

3.4.1 Setting the equations

The general action of the ESTGB theory in vacuum that has been considered in this study is the following:

$$\mathcal{S} = \frac{1}{16\pi}\int dx^4\sqrt{-g}\Big[2R - 2\Lambda - \partial_\mu\phi\partial^\mu\phi + f(\phi)I\Big] \ . \tag{3.15}$$

In this expression, the Lagrangian density does not contain only the Ricci curvature (as in the original Einstein-Hilbert action) but also the cosmological constant, Λ, the

[2]Differentiable manifold with a metric tensor that defines a positive inner product on the tangent space of each point.

kinetic term of the scalar field, $\partial_\mu\phi\partial^\mu\phi$, and a higher-order curvature term non-minimally coupled to a function of the spin-0 field. This coupling is needed, otherwise, the GB invariant, I, would not enter the dynamics and, in 4D, its contribution to EOM would just vanish. Indeed, the integral of the GB invariant would be equal to a constant with a value that depends on the Euler characteristic[3] of the manifold and its contribution would tend to zero upon extremization. As has already been mentioned above (see Sec. 1, the coupling function considered is non-linear:

$$f(\phi) = \beta\phi^4 \ . \tag{3.16}$$

By varying the action in Eq. 3.15 with respect to the metric tensor $g_{\mu\nu}$ and the scalar field ϕ it is possible to obtain respectively the gravitational field equations and the equation for the scalar field:

$$G_{\mu\nu} + \Lambda g_{\mu\nu} = R_{\mu\nu} - \frac{1}{2}g_{\mu\nu}R + \Lambda g_{\mu\nu} = T_{\mu\nu} \ , \tag{3.17}$$

$$\Box\phi = -f_{,\phi}\, I \ . \tag{3.18}$$

In particular, in Eq. 3.17, $T_{\mu\nu}$ is the stress-energy tensor that takes into account the variation of the ϕ-dependent part of the action with respect to the metric, and in Eq. 3.18 $\Box$ indicates the D'Alambert operator, while $f_{,\phi}$ indicates the derivative with respect to the scalar field ϕ.

The computations that follow have been resolved using the computational software program Wolfram Mathematica [49]. Firstly, since the interest is aimed at finding regular, static, asymptotically flat BH solutions with a non-trivial scalar field, which are spherically symmetric, the appropriate metric ansatz is established. The ansatz to the solution of the second-order differential equation for the metric that can be obtained from the variation of the action with respect to the metric, using Schwarzschild-like coordinates (t, r, θ, ϕ), is

$$ds^2 = -\sigma(r)^2 H(r)dt^2 + \frac{dr^2}{H(r)} + r^2(d\theta^2 + \sin^2\theta d\varphi^2) \ , \tag{3.19}$$

$$g_{\mu\nu} = \begin{bmatrix} -\sigma(r)^2 H(r) & 0 & 0 & 0 \\ 0 & \frac{1}{H(r)} & 0 & 0 \\ 0 & 0 & r^2 & 0 \\ 0 & 0 & 0 & r^2\sin^2\theta \end{bmatrix} \ . \tag{3.20}$$

The spacetime metric is not constant but has functions that depend on the radius from the center of the coordinate system, and that describe the structure of spacetime and

[3] A topological invariant, a number that describes a topological space's shape or structure regardless of the way it is bent.

how gravity works. In particular, $H(r) = 1 - \frac{2m(r)}{r} - \frac{\Lambda r^2}{3}$ is related to the gravitational potential, while $\sigma(r)$ is associated with the energy density (everywhere equal to 1 for a BH). $H(r)$ and $\sigma(r)$ are unknowns to find. It is then computed also the determinant indicated with g, as $\sqrt{-g} = r^2\sigma(r)\sin\theta$ appears in the expression of the action. The next step is then to explicit the connection between Christoffel symbols and the metric tensor (the former is a combination of the derivatives of the latter).

In this way, it is then possible to compute all the curvature identities that compose the GB invariant: the Riemann tensor, which depends only on the Christoffel symbols as Eq. 2.3 shows, and the Ricci tensor and Ricci scalar from Riemann tensor contractions. During this computation, it has been noticed that total derivative terms in the Lagrangian density can be removed. It is a property of the variational principle the fact that the EOM do not change by adding to the functional a total derivative: in this case, applying the divergence theorem, the integral of a total derivative reduces to a boundary integral (integral in a lower dimension), but variations of the field at the boundaries are zero.

Finally, the expression of the effective Lagrangian is put together as written inside the action integral, where the scalar field ϕ also appears. Using the variational method on the effective Lagrangian it is possible to obtain the differential Euler-Lagrange equations obeyed by $H(r), \sigma(r)$ and the scalar field $\phi(r)$. The Euler-Lagrange equations for $H(r)$ and $\sigma(r)$ are exactly the Einstein field equations with the metric ansatz introduced before (Eq. 3.19) and where the stress-energy tensor takes into account the scalar field and the GB term. The modified Einstein field equations that can be obtained by varying the modified Einstein-Hilbert action with respect to the metric are therefore

$$G_{\mu\nu} + \Lambda g_{\mu\nu} - (T\phi)_{\mu\nu} - (T_{GB})_{\mu\nu} = 0 \ , \tag{3.21}$$

where $G_{\mu\nu} = R_{\mu\nu} - \frac{1}{2}g_{\mu\nu}R$ is the Einstein tensor; $(T\phi)_{\mu\nu}$ is the energy-momentum tensor of a minimally coupled scalar, and $(T_{GB})_{\mu\nu}$ represents the contribution from the GB (Eq. 3.14) term. The expression for $(T\phi)_{\mu\nu}$ is:

$$(T\phi)_{\mu\nu} = -\frac{1}{2}g_{\mu\nu}\partial_\rho\phi\partial^\rho\phi + \partial_\mu\phi\partial_\nu\phi \quad , \tag{3.22}$$

and the expression for $(T_GB)_{\mu\nu}$ is:

$$(T_{GB})_{\mu\nu} = -\frac{1}{2}(g_{\rho\mu}g_{\lambda\nu} + g_{\lambda\mu}g_{\rho\nu})\eta^{\kappa\lambda\alpha\beta}\frac{\epsilon^{\rho\gamma\omega\tau}}{\sqrt{-g}}R_{\omega\tau\alpha\beta}\nabla_\gamma\partial_\kappa f \quad , \tag{3.23}$$

(see [5]). From the computations with Wolfram Mathematica the field equations for $H(r)$ and $\sigma(r)$ are:

$$H'(r) = \frac{1 - r^2\Lambda + H(r)\{-1 - \phi'(r)^2[r^2 + 4(-1 + H(r))f''(\phi(r))] - 4(-1 + H(r)f'(\phi(r))\phi''(r)\}}{r + 2(-1 + 3H(r))f'(\phi(r))\phi'(r)} \tag{3.24}$$

$$\sigma'(r) = \frac{\sigma(r)\{\phi'(r)^2[r^2 + 2(-1 + H(r)f''(\phi(r)] + 2(-1 + H(r))f'(\phi(r))\phi''(r)\}}{r + 2(-1 + 3H(r))f'(\phi(r))\phi'(r)} \quad . \tag{3.25}$$

The EOM for the scalar field can be computed instead by varying the same action with respect to the scalar field. It is the relativistic wave equation (*aka* Klein-Gordon equation) that describes the dynamics of bosons (with spin-0). In this case:

$$\frac{1}{\sqrt{-g}}\partial_\mu\Big[g^{\mu\nu}\sqrt{-g}\partial_\nu\phi(r)\Big] - \frac{1}{4}\frac{\partial f(\phi(r))}{\partial\phi}I = 0 \ . \tag{3.26}$$

The Kretchmann scalar $R_{\mu\nu\delta\lambda}R^{\mu\nu\delta\lambda}$, the Virial identity [44] and the Smarr relation are identities used to check the numerics of the solutions. The computed Virial identity is:

$$\begin{aligned}
&\frac{-\{4\sigma(r)(r^2[-1 + r(3r - 2r_h)\Lambda] + 4(-1 + 3H(r))f'(\phi(r))^2\phi'(r)^2[1 + r(-3r + 2r_h)\Lambda}{r + 2(-1 + 3H(r))f'(\phi(r))\phi'(r))^2} + \\
&\frac{+H(r)(-2 + 6r^2\Lambda - 4rr_h\Lambda + H(r)(-1 + r(r - 2r_h)\phi'(r)^2)]]}{r + 2(-1 + 3H(r))f'(\phi(r))\phi'(r))^2} + \\
&\frac{2f'(\phi(r))\phi'(r)[2r(1 + r(-3r + 2r_h)\Lambda] + H(r)[r_h + r[-7 + r(17r - 11r_h)\Lambda]}{r + 2(-1 + 3H(r))f'(\phi(r))\phi'(r))^2} + \\
&\frac{+H(r)[r - r_h - r2(r + r_h)\phi'(r)^2)]]\}}{r + 2(-1 + 3H(r))f'(\phi(r))\phi'(r))^2} = 0 \ .
\end{aligned} \tag{3.27}$$

The Smarr formula relates the mass of the BH (M) with other physical properties like entropy, angular momentum, and electric charge. In this case, the last two properties are null, then the relation is:

$$M = 2T_H S_H + M_s \ , \tag{3.28}$$

where T_H is the Hawking temperature, M_s is the contribution of the scalar field and its coupling:

$$M_s = 4\pi\Lambda^2 f(\phi) \ . \tag{3.29}$$

The entropy S_H is calculated as:

$$S_H = \frac{1}{4}A_H = \frac{1}{4}4\pi R_H \ , \tag{3.30}$$

with R_H being the Schwarzschild radius.

3.4.2 Obtaining solutions

The search for BH solutions with a non-trivial scalar field continues by determining a set of asymptotic solutions near the event horizon (r_h) and near the cosmological horizon (r_c).

These solutions set the boundary condition for the numerical integration and constraints for the theory. Near the event horizon, $H(r_h) = 0$, it is possible to expand the metric functions and the scalar field as standard Taylor expansions for r very close to r_h:

$$\begin{aligned} \sigma(r) &= d_0 + d_1(r - r_h) + d_2(r - r_h)^2 + ... \ , \\ H(r) &= h_1(r - r_h) + h_2(r - r_h)^2 + ... \ , \\ \phi(r) &= p_0 + p_1(r - r_h) + p_2(r - r_h) + ... \ . \end{aligned} \tag{3.31}$$

It can be noticed that it has been put $h_0 = 0$. This is one of the boundary conditions that needs to be imposed since it means that $H(r = r_h) = 0$ and so that the g_{rr} component of the metric diverges, establishing at that radius the event horizon. Indeed, as already mentioned in Sec. 2.1.1, the event horizon is a coordinate singularity that covers the physical singularity. It is then possible to find the coefficients of each expansion by evaluating the power series expansion of the difference between the derivative of the expanded functions and the expressions found previously (see Sec. 3.4.1) for r very close to r_h until the first order. By doing this, for the scalar field $\phi(r)$, it turns out that there are three possibilities for the value of the variation of the scalar field at the event horizon r_h (polynomial equation of third grade in p_1):

$$p_1 = \frac{1}{2f_{,\phi}\left(p_0\right)} \ , p_1 = \frac{1 - \sqrt{1 - 24f_{,\phi}\left(p_0\right)^2}}{4f_{,\phi}\left(p_0\right)} \ , p_1 = \frac{1 + \sqrt{1 - 24f_{,\phi}\left(p_0\right)^2}}{4f_{,\phi}\left(p_0\right)} \ . \tag{3.32}$$

The first term makes every contribution from $H(r)$ equal to zero, the second one makes the field grow, which can be considered not physical, and finally, the third one is the correct one to consider because makes the scalar field decay. One constraint on the form of the coupling function arises from the demand that the first derivative of the scalar field on the horizon must be real, meaning that the term under square root must be positive. It can also be noticed that to simplify this computation, it can be put $r_h = 1$, which fixes the scale. Indeed BHs are scale-invariant, meaning that the physics that describes them is independent of their size.

Finally, all the coefficients of the expansions are obtained as functions of the parameters d_0 and p_0, respectively the amplitude of $\sigma(r)$, and the scalar field at the event horizon:

$$h_1 = -\frac{1}{2p_1 f_{,\phi}\left(p_0\right)} \ , \tag{3.33}$$

$$d_1 = \frac{d_0 p_1 f, _{,\phi}\left(p_0\right)}{f_{,\phi}\left(p_0\right)} \ . \tag{3.34}$$

The parameter d_0 is obtained from the numerics, while p_0 is an unknown parameter of a boundary value problem: p_0 is solved by a numerical method that chooses the correct value that makes the two boundary conditions (BC) to be obeyed. In this case, the boundary conditions are $H(r_c) = H(r_h) = 0$ and have a scalar field that is finite and

smooth at those horizons. Eqs. 3.31 define a BH horizon with a regular scalar field, provided that conditions on p_1 and the coupling function are satisfied. The same can be done for $r = r_c$= cosmological horizon, explaining the expansions of the metric functions and the scalar field:

$$\begin{aligned} \sigma(r) &= d_c + d_1(r - r_c) + d_2(r - r_c)^2 + ... \ , \\ H(r) &= h_1(r - r_c) + h_2(r - r_c)^2 + ... \ , \\ \phi(r) &= p_c + p_1(r - r_c) + p_2(r - r_c) + ... \ , \end{aligned} \tag{3.35}$$

where again imposing $H(r = r_c) = 0$ is equivalent to establish the cosmological horizon at $r = r_c$ as a boundary condition. The method that has been followed to find the coefficients is the same as above: the power series to the first order of the difference between the derivative of the expansions around r_c and the expressions found previously (see Sec. 3.4.1), always in r_c, are computed. Then, by equalizing their expressions to zero it is possible to obtain a formulation for the coefficients of the expansions around r_c. Thus, the following expressions for the coefficient were found:

$$h_1 = \frac{1}{r_c - 2p_1 f_{,\phi}(p_c)} \ , \tag{3.36}$$

$$d_1 = \frac{d_0 p_1^2 (r_c^2 - 2f, _{,\phi}(p_c))}{r_c - 2p_1 f_{,\phi}(p_c)} \ , \tag{3.37}$$

$$p_1 = \frac{r_c}{2f_{,\phi}(p_c)} \ , p_1 = \frac{r_c^2 - \sqrt{r_c^6 - 24 r_c^2 f_{,\phi}(p_c)^2}}{4 r_c^2 f_{,\phi}(p_c)} \ , p_1 = \frac{r_c^3 + \sqrt{r_c^6 - 24 r_c^2 f_{,\phi}(p_c)^2}}{4 r_c^2 f_{,\phi}(p_c)} \ . \tag{3.38}$$

The construction of the asymptotic solution at r_h and r_c can give valuable insight into understanding the solution. However, due to the complexity of the equations, only through numerical integration it will be possible to search for solutions that obey the smooth connection.

Once the expression for $H'(r)$, $\sigma'(r)$ and $\phi''(r)$ are obtained, their integration must be computed through numerical methods since $H(r)$, $\sigma(r)$, $\phi(r)$ do not have known analytical form. The method used to integrate is Runge-Kutta, while the secant method is used as a Shooting method to guarantee that the solution obeys the boundary condition. The Runge-Kutta method is a numerical method used to solve complicated differential equations coming from mathematical and physical models. Given the value of a certain function at a starting point and given its derivative, it calculates the function in a success of points using calculations of the derivatives in intermediate points. These intermediate points are used to find out the tendency, and the value of the function in one step away from the starting point is a weighted average of the derivative of the function in these intermediate points. In such way, $\phi(r)''$, $H'(r)$ and $\sigma'(r)$ are integrated recursively from a certain radial coordinate value r_n to the point that is one step away, r_{n+1}, with the Runge-Kutta method (imagining to discretize the integration interval in a

1D grid). The order of the Runge-Kutta method determines its accuracy and how many intermediate points have been used. The Runge-Kutta method of first order can be reduced to the Euler method, and the Heun's method can be thought of as a second-order Runge-Kutta; including more trial steps, the method becomes more accurate, meaning that the local and total truncation error becomes smaller. The most known member of the Runge-Kutta family is the 4^{th} order Runge-Kutta method. Supposing that we have a differential equation of the type $y' = f(t, y)$, then y_{n+1} given below is the approximation for $y(t_{n+1})$ given by this numerical method (see Fig.3.1):

$$y_{n+1} = y_n + \frac{h}{6}(k_1 + 2k_2 + 2k_3 + k_4) \ , \tag{3.39}$$

where h is the step such that $t_{n+1} = t_n + h$ and k_i are the various slopes given by

$$\begin{aligned} k_1 &= f(t_n, y_n) \ , \\ k_2 &= f(t_n + \frac{h}{2}, y_n + h\frac{k_1}{2}) \ , \\ k_3 &= f(t_n + \frac{h}{2}, y_n + h\frac{k_2}{2}) \ , \\ k_4 &= f(t_n + h, y_n + hk_3) \ . \end{aligned} \tag{3.40}$$

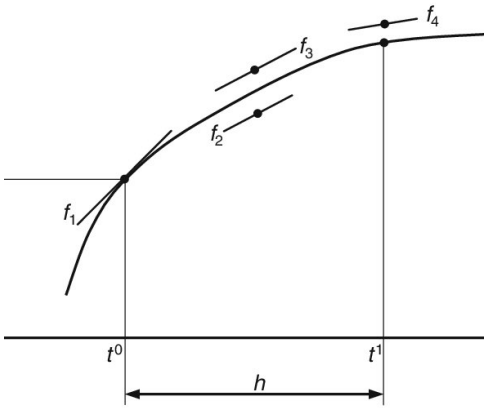

Figure 3.1: The image shows the slopes used in the four stages of the 4^{th} Runge-Kutta method: the derivative of the function at the starting point, the derivative at the middle point, firstly calculated from the starting point, then calculated using the slope obtained at the previous step, finally the derivative calculated at the ending point.

The fact that is a 4^{th} order method means that the total accumulated error is on the order of $\mathcal{O}(h^4)$. The coefficients are found by imposing algebraic conditions, known as order conditions, that ensure the method accurately approximates the solution in the prescribed order. The various derivatives at the intermediate points are calculated iteratively from the previous point's calculations, with the effect of gaining more accuracy. The largest weights are given to the derivatives calculated at the midpoint. For a general Runge-Kutta method, the expression for the next value computation becomes

$$y_{n+1} = y_n + h \sum_{i=1}^{s} b_i k_i \ , \tag{3.41}$$

where h is the step size, s indicates the number of intermediate stages, b_i are the weights associated to each stage and k_i represent the intermediate slope:

$$k_i = f\left(t_n + c_i h, y_n + h \sum_{j=1}^{i-1} a_{ij} k_j\right) \quad \text{for} \quad i = 1, 2, \ldots, s \ . \tag{3.42}$$

The coefficients a_{ij}, c_i can be derived from the Butcher tableau. For a further presentation on the topic of differential equations and the Runge-Kutta method see [23]. Since the problem is tackled through several steps, often a balance between accuracy and computational time is required, which is not established a priori but depends on the problem.

In particular, in this case, they have been used the 5^{th} and 6^{th} order Runge-Kutta methods (respectively with six and seven stages) with an adaptive step size. This means that the step between the two points in which the function is calculated can be very big if, in that region, the function is constant, while it must be very small if the function oscillates a lot to correctly describe the intricate profile. The more suitable step is found by evaluating the difference between 5^{th} and 6^{th} Runge-Kutta methods and evaluating whether it is less than the established tolerance. Once the biggest step under the accuracy is found, $\phi(r)$, $\phi'(r)$, $H(r)$, and $\sigma(r)$ are obtained in the point that is one step away from the previous. Then the cycle continues considering what's just calculated as the starting values for the next iteration. The integration goes on from the Schwarzschild radius (r_h) to the cosmological horizon (r_c), hence until $H(r) = 0$ that is the boundary condition for the cosmological horizon. The integration then continues from there to two times the cosmological horizon as a guarantee of the correct asymptotic behavior.

The computation of this integration gives a result in the profiles $\phi(r)$, $H(r)$, $\sigma(r)$ (see Fig. 3.2), and the aim of the Shooting method is then to guarantee the boundary conditions at r_h and r_c. Indeed, guessed a value for ϕ_0 to integrate (value of the scalar field at r_h), the value obtained for ϕ_c (value of the scalar field at r_c) after the integration has to be equal to the expectations and it has to be continuous at r_c. If it is not, then a new initial condition ϕ_0 is injected by the Shooting method into the integration and

this cycle can finish when the boundary conditions are obeyed. The method used to compute the new guess for ϕ_0 from the previous ones is the secant method (*aka* discrete Newton's method), a recursive algorithm to find the roots of a function. In this case, the secant method is used to find the roots of the function given by the difference between $pf = 1E-6$ and pt. The latter is a difference between two values of the first derivative of the scalar field at the cosmological horizon, the one obtained from the integration until r_c and the one obtained instead from its expression calculated in the value of r_c resulting from the integration. The value of ϕ_0 is changed in each iteration, obtained from the two guesses before using the secant method. It is indeed found as the variable for which the function goes to zero and so the cycle of the Shooting method finishes when $pf - pt < tolerance$.

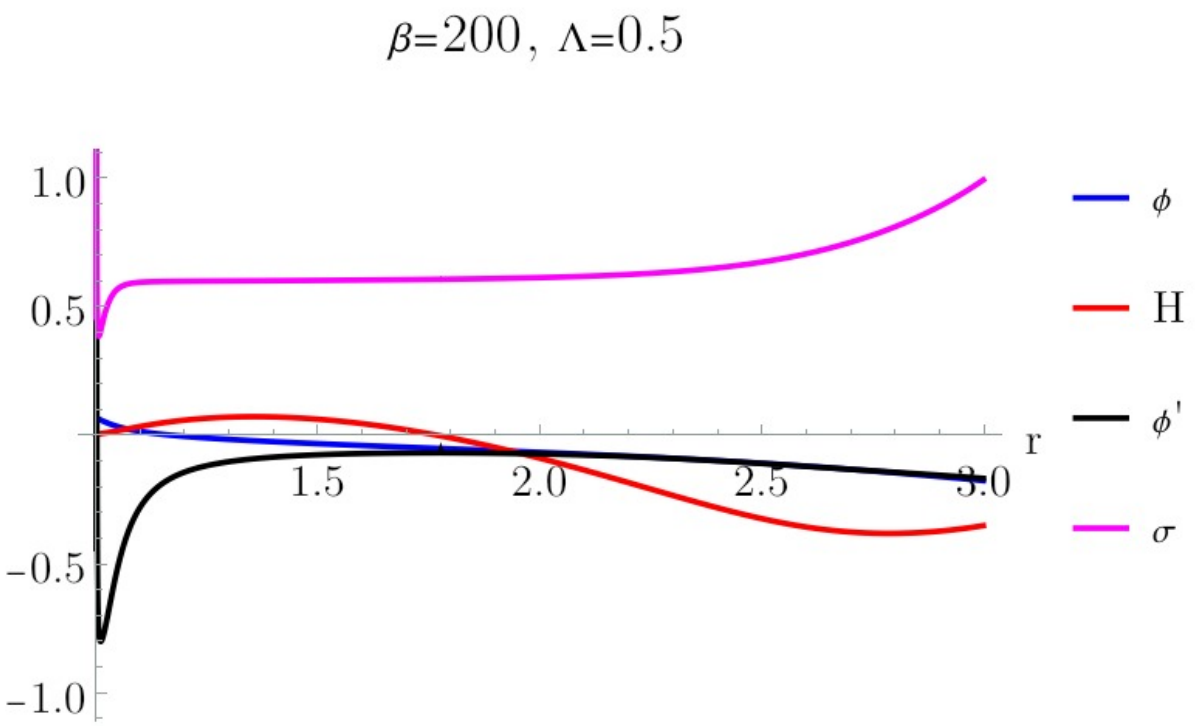

Figure 3.2: The trends as functions of r, obtained from the numerical integration, with a fixed value of β and λ, parameters of the integration

Fig. 3.2 shows how the profile of $H(r)$ (red) has two nodes (intersection with the radial axis) at values $r = 1r_h$ and $r = 1.8r_h$, thus indicating the value of the radial coordinate for the Schwarzschild radius and for the cosmological horizon. At the same time, the scalar field (blue) presents one node more or less at value $r = 1.2r_h$ and the stronger decrease near small values of r, as can be seen from the derivative (black). In particular,

it does not vanish at the r_c pointed out by $H(r)$, a sign of the scalarization it suffers. This could indicate a probable contribution of the scalar field to the dynamics of the Universe. As expected from the profile of the scalar field, its first derivative (black) is steep for small values of r where the scalar field decreases more rapidly. By varying the value of the coupling constant β and Λ, various profiles for the scalar field in the function of the coordinate r were obtained, such as the one in Fig. 3.2.

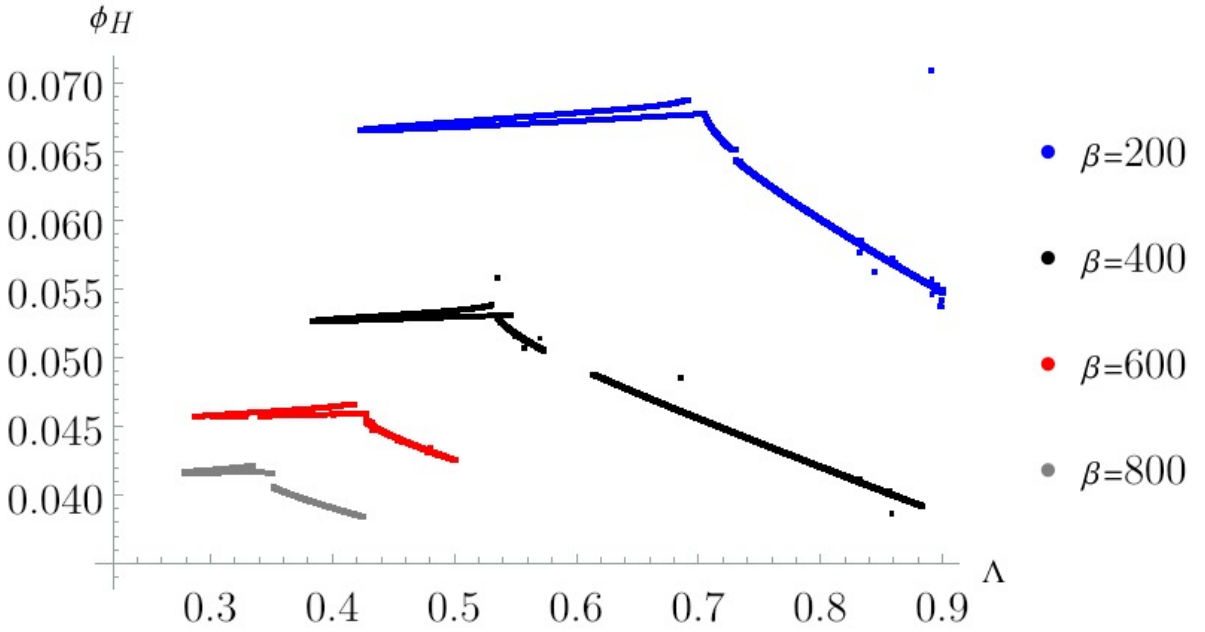

Figure 3.3: Domain of existence: each curve is for a different value of β, where it is possible to recognize the two branches of scalarized solutions. In particular, it can be noticed that the branches are more extended for smaller values of β and that the "turning point" is found at increasing values of Λ.

For a fixed β, they have been collected values of p_0, p_c, Λ and r_c (there is always $r_h = 1$ fixed) and they have been used to build some plots with Wolfram Mathematica tool, such as the BHs evolutionary branches $\phi_0(\Lambda)$ (see Fig. 3.3, ϕ_H and ϕ_0 are used with the same meaning and they correspond to p_0 in the code used for calculations, representing the physical quantity of the scalar field at the Schwarzschild radius r_h). Indeed these latter show two branches that stand for the two scalarized solutions expected by the non-linear scalarization. The smaller β, the more extended the branches of solutions, meaning the scalar field can undergo scalarization over a broader range of Λ. Since β represents the strength of the coupling between the scalar field and the GB curvature term, a smaller β

leads to a weaker influence of the curvature on the scalar field configuration. This makes it possible to have a non-trivial scalar field configuration even far away from the source of strong curvature. Moreover, a bigger Λ indicates a more rapid expansion. Thus, a bigger value of the scalar field at the Schwarzschild radius would be required to have a scalar field even at the cosmological horizon. From those, it has been searched for the "turning point" that in turn corresponds to the minimum Λ for which the curvature of the De Sitter spacetime[4] is sufficient to produce a non-trivial scalar configuration. Indeed, scalarization is mainly driven by the combined action of the three parameters β, Λ, and the BH mass/radii. The quartic function considered has introduced a non-linear interaction between the scalar field and the curvature, where the coupling constant β determines the strength of the interaction between the scalar field and the GB term: higher β means stronger coupling. At the same time, as the cosmological constant increases, the overall curvature of the spacetime also increases.

Once the minimum Λ and the corresponding r_c, p_0, and p_c have been obtained for each β, it has been underlined the correlation between each of them and β (see Fig. 3.4, Fig. 3.5, Fig. 3.6, Fig. 3.7).

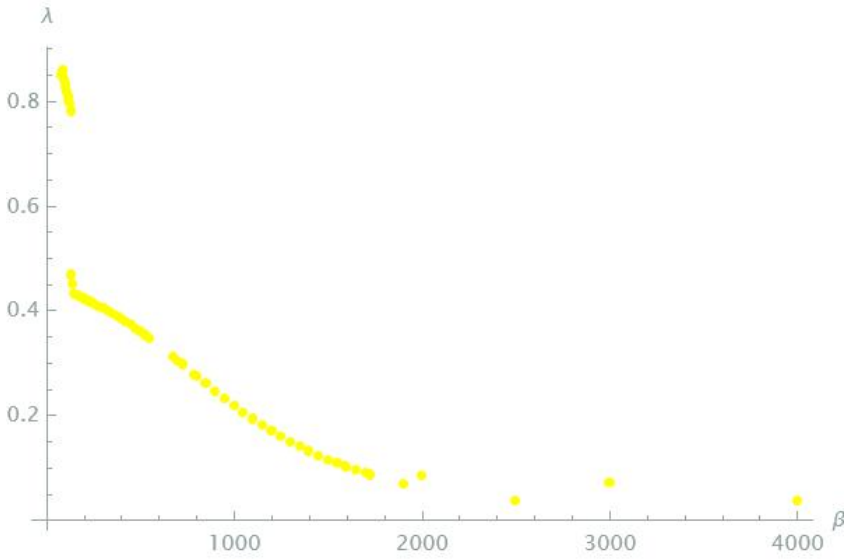

Figure 3.4: Relation between the cosmological constant, Λ, and the coupling constant of the quartic coupling function, β. In particular, for each β, the value of Λ is the minimum able to induce scalarization.

[4]De Sitter space is the maximally symmetric vacuum solution of Einstein's field equations with a positive cosmological constant Λ (which corresponds to a positive vacuum energy density and negative pressure). It is the simplest cosmological model consistent with the observed accelerated expansion of the Universe. The curvature of De Sitter space is directly connected to the cosmological constant through $R = 4\Lambda$.

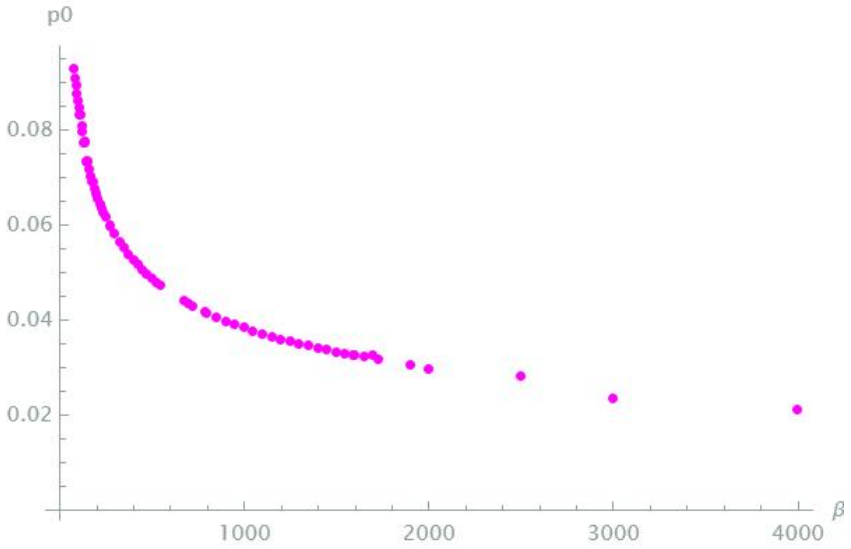

Figure 3.5: Relation between the value of the scalar field at the Schwarzschild horizon, p_0, and the coupling parameter, β.

Of particular interest is the correlation between the cosmological constant Λ and the coupling constant β; indeed, an increasing Λ corresponds to a decreasing β. This means that if Λ grows, then also the acceleration that it drives increases, and the cosmological horizon[5] shrinks. Consequently, a minor β is needed to have the same level of scalarization. This can be summarized by saying that the minimum Λ gives the largest possible cosmological horizon able to endow scalarization: a smaller Λ means a slower rate of acceleration, allowing the universe to expand more before the horizon is reached. This results in a larger observable universe.

The fact that this minimum value of Λ is larger for a smaller value of β is in accordance also with the considerations of Fig. 3.3. The value of the scalar field at the Schwarzschild radius corresponding to that minimum value of Λ is plotted in Fig. 3.5. This latter shows a clear and regular decrease. Indeed, it is reasonable to think that the amplitude of the scalar field, the shooting parameter of the integration, should be larger when the coupling to the curvature is weaker, in order to maintain the same level of scalarization. Developing the integration, the values of the scalar field at the cosmological horizon will then be bigger in absolute value (more negative, see also Fig. 3.2) for smaller values of the coupling constant β, since these latter are associated to a bigger value of Λ and so to a smaller cosmological horizon. This is what can be seen in Fig. 3.6. Finally, Fig. 3.7 shows how the cosmological horizon shrinks for smaller values of β, while it enlarges as β increases: a great value of Λ indicates a greater acceleration, making the observable

[5]The cosmological horizon is defined as the maximum distance from which light or any other form of radiation can reach an observer. It is also known as De Sitter horizon.

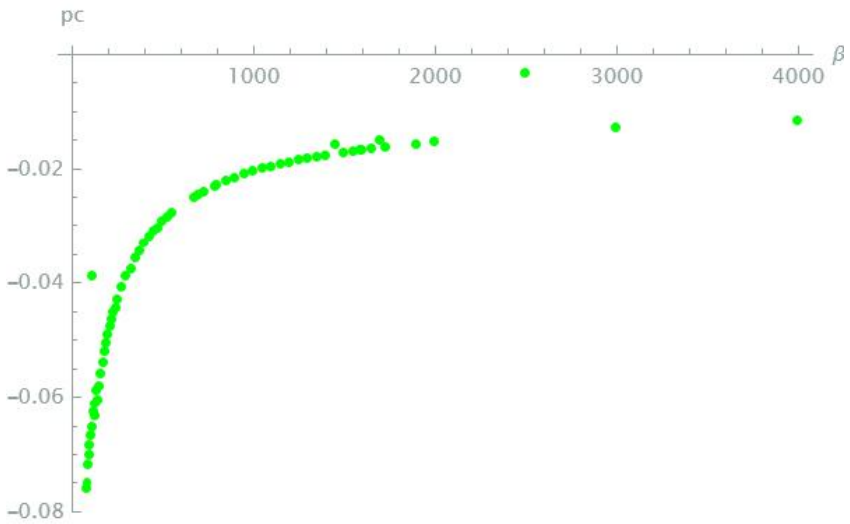

Figure 3.6: Relation between the value of the scalar field at the cosmological horizon, p_c, and the coupling parameter β.

Universe smaller. Then, in order to have a scalarized cosmological horizon, the largest possible, a smaller value of β is required. The value of r_c plotted represents for each β the largest cosmological horizon possible. However, it presents more discontinuity with respect to the plots above, especially for the extremal values of β. This can be a symptom of the presence of a different behavior for the scalar field in these extreme conditions or a reduced efficiency of the numerical methods used to integrate.

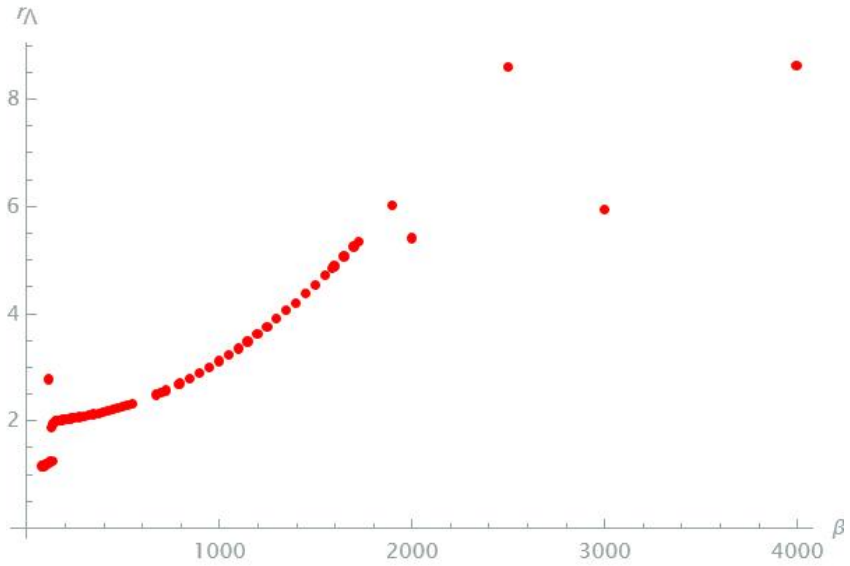

Figure 3.7: Relation between the radial coordinate of the cosmological horizon, r_Λ, and the coupling parameter, β.

Chapter 4

Conclusion

The purpose of this essay was to study the scalarization of the cosmological horizon in the context of ESTGB theory with a quartic coupling function $f(\phi) = \beta\phi^4$. First, the modified Einstein field equations and the EOM for the scalar field have been obtained for this theory. Proceeding by integration with the use of the numerical method Runge-Kutta and the secant method as the Shooting method, it has been possible to further obtain the profile of the scalar field as a function of the radial coordinate, from the Schwarzschild radius to the cosmological horizon, for different values of the cosmological constant Λ and β.

For each β it has also been plotted the values of the scalar field at the Schwarzschild horizon corresponding to different cosmological constant values. After locating the two non-trivial solutions for the scalar field expected by a non-linear interaction with the GB term, it has been searched for the minimum value of the cosmological constant which endows scalarization. Finally, it has been collected for each β this precise value of Λ together with the corresponding values of p_0, p_c, and r_c. This has made it possible to compare the results produced and obtain different scenarios.

This study comes with the recent efforts that modern Astrophysics and Cosmology are making to explain the mystery of DE and DM. Identifying the behavior of the scalar field with variations of Λ and β can be interesting in developing a more profound understanding of the relation between geometry and field dynamics in such scalar-tensor theories as ESTGB. The presence of the scalar field could contribute to the accelerated expansion of the Universe and to its overall content, possibly mimicking DM and DE. Indeed it is expected for the scalar field to alter the effect of the cosmological constant and to influence the large-scale structure of the Universe. The physics field of modified gravity is elaborating many new and different models that, at least from a theoretical point of view, introduce deviation from GR. Hopefully, in the future, the scientific community will be able to detect such deviations due to new fundamental fields. More precisely, it has already been mentioned how scalar fields could leave their imprints on extremely compact objects. At the level of cosmological observations instead, not only

the Cosmic Microwave Background (CMB) could hide clues about scalar fields (Simons Observatory and CMB-S4 [1] would provide precise surveys of the CMB), but also cosmic structures can be influenced by the presence of scalar fields and so observations of galaxy and cluster distribution and other large-scale structures can lead to discoveries (Dark Energy Spectrum Instrument - DESI [88] - and Euclid mission will map the large-scale structures of the universe with an unexperienced detail). At the moment LIGO (ground-based detector) and LISA (space-based detector that will be launched in 2035) interferometers are among the greatest observational projects to measure the presence of non-trivial scalar field through gravitational wave signals [63]. In particular, LISA will be able to detect gravitational waves emitted from Extreme Mass Ratio Inspirals, where a lighter object orbits around a much heavier object. Since the additional scalar field that surrounds compact objects is strictly connected to gravity, it is expected to leave imprints on gravitational waves emitted during the inspiral. Detecting its effect and deviations from GR would be a turning point in favor of the scalar-tensor theories. Moreover, as many different scalar-tensor theories exist, confronting the observed parameters (in this case they would be parameters that characterized gravitational waves) with the predicted ones it should be possible to constrain those parameters and test the validity of different theories [11].

Challenges in the field of scalar-tensor theories and scalarization models come from the importance of finding a way to suitably reproduce the evolution of the observed Universe, from the inflationary scenario of the early Universe, through the evolution of perturbations until the formation of the current large-scale structure. This can lead in particular to the necessity of finding constraints on such theories. Cosmological models built on such theories could furnish alternative explanations to the current observational picture. Future attempts will also regard the exploration of whether and how scalar fields can be candidates for DM and DE. Another possibility is to study generalizations to other fields, such as vectorial or tensorial (vectorization and tensorization). This however comes with the difficulty to control extra degrees of freedom. Furthermore, studies of scalarization on compact objects such as neutron stars and BHs have inspired the exploration of the effects of putting together scalarization models in more complex astrophysical scenarios. Studies on scalarization as an effect of scalar-tensor theories can be expanded by considering different ways of igniting it and its behavior on different types of BHs (*e.g.* charged, spinning, or both, consider non-zero potential for the scalar field, effects of mass). Through theoretical studies and numerical simulations, the possible descriptions of our Universe extend, offering predictions that remain to be tested and constrained with future observations.

Bibliography

[1] Kevork N Abazajian et al. "CMB-S4 science book". In: *arXiv preprint arXiv:1610.02743* (2016).

[2] B. P. Abbott et al. "GW151226: Observation of Gravitational Waves from a 22-Solar-Mass Binary Black Hole Coalescence". In: *Phys. Rev. Lett.* 116 (24 June 2016), p. 241103. DOI: 10.1103/PhysRevLett.116.241103. URL: https://link.aps.org/doi/10.1103/PhysRevLett.116.241103.

[3] N. Aghanim et al. "Planck2018 results: VI. Cosmological parameters". In: *Astronomy amp; Astrophysics* 641 (Sept. 2020), A6. ISSN: 1432-0746. DOI: 10.1051/0004-6361/201833910. URL: http://dx.doi.org/10.1051/0004-6361/201833910.

[4] Lorenzo Annulli, Carlos AR Herdeiro, and Eugen Radu. "Spin-induced scalarization and magnetic fields". In: *Physics Letters B* 832 (2022), p. 137227.

[5] G Antoniou, A Bakopoulos, and P Kanti. "Evasion of no-hair theorems and novel black-hole solutions in Gauss-Bonnet theories". In: *Physical review letters* 120.13 (2018), p. 131102.

[6] George Antoniou, A Bakopoulos, and P Kanti. "Black-hole solutions with scalar hair in Einstein-scalar-Gauss-Bonnet theories". In: *Physical Review D* 97.8 (2018), p. 084037.

[7] Keiichi Asada and Masanori Nakamura. "First Results of the Event Horizon Telescope". In: 2020. URL: https://api.semanticscholar.org/CorpusID:234947045.

[8] DUMITRU Astefanesei et al. "Einstein-Maxwell-scalar black holes: classes of solutions, dyons and extremality". In: *Journal of High Energy Physics* 2019.10 (2019), pp. 1–27.

[9] Pierre Astier. "The expansion of the universe observed with supernovae". In: *Reports on Progress in Physics* 75 (2012). URL: https://api.semanticscholar.org/CorpusID:140756.

[10] Athanasios Bakopoulos, George Antoniou, and Panagiota Kanti. "Novel black hole solutions with scalar hair in Einstein-scalar-Gauss-Bonnet theories". In: *AIP Conference Proceedings*. Vol. 2075. 1. AIP Publishing. 2019.

[11] Susanna Barsanti et al. "Extreme mass-ratio inspirals as probes of scalar fields: Eccentric equatorial orbits around Kerr black holes". In: *Physical Review D* 106.4 (2022), p. 044029.

[12] Jacob D Bekenstein. "Black holes: classical properties, thermodynamics and heuristic quantization". In: *arXiv preprint gr-qc/9808028* (1998).

[13] Jacob D Bekenstein. "Transcendence of the law of baryon-number conservation in black-hole physics". In: *Physical Review Letters* 28.7 (1972), p. 452.

[14] VA Belinsky et al. *Inflationary stages in cosmological models with a scalar field.* Tech. rep. International Centre for Theoretical Physics, 1985.

[15] Zakaria Belkhadria and Alexandre M Pombo. "Mixed scalarization of charged black holes: From spontaneous to nonlinear scalarization". In: *Physical Review D* 110.4 (2024), p. 044014.

[16] Emanuele Berti et al. "Spin-induced black hole scalarization in einstein-scalar-gauss-bonnet theory". In: *Physical Review Letters* 126.1 (2021), p. 011104.

[17] Emanuele Berti et al. "Testing general relativity with present and future astrophysical observations". In: *Classical and Quantum Gravity* 32.24 (2015), p. 243001.

[18] Jose Luis Blázquez-Salcedo et al. "Einstein-Maxwell-scalar black holes: the hot, the cold and the bald". In: *Physics Letters B* 806 (2020), p. 135493.

[19] Jose Luis Blázquez-Salcedo et al. "Quasinormal modes of hot, cold and bald Einstein–Maxwell-scalar black holes". In: *The European Physical Journal C* 81 (2021), pp. 1–16.

[20] Carson Blinn. *Schwarzschild Solution to Einstein's General Relativity.* 2017.

[21] Yves Brihaye and Betti Hartmann. "Spontaneous scalarization of charged black holes at the approach to extremality". In: *Physics Letters B* 792 (2019), pp. 244–250.

[22] Niccolo Bucciantini and Jacopo Soldateschi. "Iron line from neutron star accretion discs in scalar tensor theories". In: *Monthly Notices of the Royal Astronomical Society: Letters* 495.1 (2020), pp. L56–L60.

[23] John C. Butcher. "The numerical analysis of ordinary differential equations: Runge-Kutta and general linear methods". In: *Mathematics of Computation* 51 (1987), p. 377. URL: `https://api.semanticscholar.org/CorpusID:121057780`.

[24] Salvatore Capozziello, Vincenzo Fabrizio Cardone, and A Troisi. "Dark energy and dark matter as curvature effects?" In: *Journal of Cosmology and Astroparticle Physics* 2006.08 (2006), p. 001.

[25] Roberto Casadio. *Elements of General Relativity.* Appunti del corso tenuto presso l'Università di Bologna. 2024.

[26] Peter Coles. "Einstein, Eddington and the 1919 eclipse". In: *Historical development of modern cosmology*. Vol. 252. 2001, p. 21.

[27] ATLAS Collaboration. "Observation of a new particle in the search for the Standard Model Higgs boson with the ATLAS detector at the LHC". In: *Physics Letters B* 716 (2012), pp. 1–29.

[28] The Event Horizon Telescope Collaboration. "First M87 Event Horizon Telescope Results. I. The Shadow of the Supermassive Black Hole". In: 2019. URL: https://api.semanticscholar.org/CorpusID:260584657.

[29] Lucas G Collodel et al. "Spinning and excited black holes in Einstein-scalar-Gauss–Bonnet theory". In: *Classical and Quantum Gravity* 37.7 (2020), p. 075018.

[30] Pedro VP Cunha, Carlos AR Herdeiro, and Eugen Radu. "Spontaneously scalarized Kerr black holes in extended scalar-tensor–Gauss-Bonnet gravity". In: *Physical Review Letters* 123.1 (2019), p. 011101.

[31] Mariafelicia De Laurentis, Paolo Pani, and Michele Punturo. "Einstein's Theory at the Extremes: Gravitational Waves and Black Holes". In: *New Challenges and Opportunities in Physics Education*. Ed. by Marilena Streit-Bianchi et al. Cham: Springer Nature Switzerland, 2023, pp. 81–92. ISBN: 978-3-031-37387-9. DOI: 10.1007/978-3-031-37387-9_6. URL: https://doi.org/10.1007/978-3-031-37387-9_6.

[32] Pacôme Delva et al. "Gravitational redshift test using eccentric Galileo satellites". In: *Physical review letters* 121.23 (2018), p. 231101.

[33] Alexandru Dima et al. "Spin-induced black hole spontaneous scalarization". In: *Physical Review Letters* 125.23 (2020), p. 231101.

[34] Marcin Domagała et al. "Gravity quantized: loop quantum gravity with a scalar field". In: *Physical Review D—Particles, Fields, Gravitation, and Cosmology* 82.10 (2010), p. 104038.

[35] Daniela D Doneva and Stoytcho S Yazadjiev. "Beyond the spontaneous scalarization: New fully nonlinear mechanism for the formation of scalarized black holes and its dynamical development". In: *Physical Review D* 105.4 (2022), p. L041502.

[36] Daniela D Doneva and Stoytcho S Yazadjiev. "New Gauss-Bonnet black holes with curvature-induced scalarization in extended scalar-tensor theories". In: *Physical review letters* 120.13 (2018), p. 131103.

[37] Daniela D Doneva et al. "Black hole scalarization induced by the spin: 2+ 1 time evolution". In: *Physical Review D* 102.10 (2020), p. 104027.

[38] Daniela D Doneva et al. "Orbital and epicyclic frequencies around rapidly rotating compact stars in scalar-tensor theories of gravity". In: *Physical Review D* 90.4 (2014), p. 044004.

[39] Pedro GS Fernandes et al. "Spontaneous scalarisation of charged black holes: coupling dependence and dynamical features". In: *Classical and Quantum Gravity* 36.13 (2019), p. 134002.

[40] Yasunori Fujii. "Cosmological Constant, Quintessence and Scalar-Tensor Theories of Gravity". In: *arXiv: General Relativity and Quantum Cosmology* (2000). URL: https://api.semanticscholar.org/CorpusID:16523006.

[41] Draen Glavan and Chunshan Lin. "Einstein-Gauss-Bonnet Gravity in Four-Dimensional Spacetime." In: *Physical review letters* 124 8 (2019), p. 081301. URL: https://api.semanticscholar.org/CorpusID:148573117.

[42] F Siddhartha Guzmán and Tonatiuh Matos. "Scalar fields as dark matter in spiral galaxies". In: *Classical and Quantum Gravity* 17.1 (2000), p. L9.

[43] Stephen William Hawking and Roger Penrose. "The singularities of gravitational collapse and cosmology". In: *Proceedings of the Royal Society of London. A. Mathematical and Physical Sciences* 314 (1970), pp. 529–548. URL: https://api.semanticscholar.org/CorpusID:120208756.

[44] Carlos A. R. Herdeiro et al. *Virial identities in relativistic gravity: 1D effective actions and the role of boundary terms*. May 17, 2017.

[45] Carlos AR Herdeiro, Alexandre M Pombo, and Eugen Radu. "Aspects of Gauss-Bonnet scalarisation of charged black holes". In: *Universe* 7.12 (2021), p. 483.

[46] Carlos AR Herdeiro et al. "Spin-induced scalarized black holes". In: *Physical review letters* 126.1 (2021), p. 011103.

[47] Shahar Hod. "Onset of spontaneous scalarization in spinning Gauss-Bonnet black holes". In: *Physical Review D* 102.8 (2020), p. 084060.

[48] Bruce Hoeneisen. "A Study of Dark Matter with Spiral Galaxy Rotation Curves". In: *International Journal of Astronomy and Astrophysics* (2019). URL: https://api.semanticscholar.org/CorpusID:155132919.

[49] Wolfram Research Inc. *Mathematica, Version 14.1*. Champaign, IL, 2024. URL: https://www.wolfram.com/mathematica.

[50] Philippe Jetzer et al. "Black holes, gravitational waves and fundamental physics: a roadmap". In: *arXiv* 1806.05195 (2018).

[51] Shun Jiang. "Spontaneous scalarization of charged Gauss-Bonnet black holes: Analytic treatment". In: *arXiv preprint arXiv:2011.03998* (2020).

[52] P. Kanti et al. "Dilatonic black holes in higher curvature string gravity". In: *Phys. Rev. D* 54 (8 Oct. 1996), pp. 5049–5058. DOI: 10.1103/PhysRevD.54.5049. URL: https://link.aps.org/doi/10.1103/PhysRevD.54.5049.

[53] Panagiota Kanti et al. "Dilatonic black holes in higher curvature string gravity". In: *Physical Review D* 54.8 (1996), p. 5049.

[54] Panagiota Kanti et al. "Dilatonic black holes in higher curvature string gravity. II. Linear stability". In: *Physical Review D* 57.10 (1998), p. 6255.

[55] Burkhard Kleihaus, Jutta Kunz, and Eugen Radu. "Rotating black holes in dilatonic Einstein-Gauss-Bonnet theory". In: *Physical Review Letters* 106.15 (2011), p. 151104.

[56] AS Koshelev, K Sravan Kumar, and P Vargas Moniz. "Inflation from string field theory". In: *arXiv preprint arXiv:1604.01440* (2016).

[57] PS Laplace. *Expositions du système du monde Imprimerie Cercle-Social*. 1796.

[58] David Lovelock. "The Einstein Tensor and Its Generalizations". In: *Journal of Mathematical Physics* 12 (1971), pp. 498–501. URL: https://api.semanticscholar.org/CorpusID:122221779.

[59] David Lovelock. "The Einstein tensor and its generalizations". In: *Journal of Mathematical Physics* 12.3 (1971), pp. 498–501.

[60] Lee C Loveridge. "Physical and geometric interpretations of the Riemann tensor, Ricci tensor, and scalar curvature". In: *arXiv preprint gr-qc/0401099* (2004).

[61] Hugh Luckock and Ian Moss. "Black holes have skyrmion hair". In: *Physics Letters B* 176.3 (1986), pp. 341–345. ISSN: 0370-2693. DOI: https://doi.org/10.1016/0370-2693(86)90175-9. URL: https://www.sciencedirect.com/science/article/pii/0370269386901759.

[62] Caio FB Macedo et al. "Self-interactions and spontaneous black hole scalarization". In: *Physical Review D* 99.10 (2019), p. 104041.

[63] Andrea Maselli et al. "Detecting fundamental fields with LISA observations of gravitational waves from extreme mass-ratio inspirals". In: *Nature Astronomy* 6.4 (2022), pp. 464–470.

[64] Eduard Massó, Francesc Rota, and Gabriel Zsembinszki. "Scalar field oscillations contributing to dark energy". In: *Physical Review D—Particles, Fields, Gravitation, and Cosmology* 72.8 (2005), p. 084007.

[65] Tonatiuh Matos, F Siddhartha Guzmán, and L Arturo Urena-López. "Scalar field as dark matter in the universe". In: *Classical and Quantum Gravity* 17.7 (2000), p. 1707.

[66] Raissa FP Mendes and Tulio Ottoni. "Scalar charges and pulsar-timing observables in the presence of nonminimally coupled scalar fields". In: *Physical Review D* 99.12 (2019), p. 124003.

[67] John Michell. "Vii. on the means of discovering the distance, magnitude, &c. of the fixed stars, in consequence of the diminution of the velocity of their light, in case such a diminution should be found to take place in any of them, and such other data should be procured from observations, as would be farther necessary for that purpose. by the rev. john michell, bdfrs in a letter to henry cavendish, esq. frs and as". In: *Philosophical transactions of the Royal Society of London* 74 (1784), pp. 35–57.

[68] Masato Minamitsuji and Taishi Ikeda. "Scalarized black holes in the presence of the coupling to Gauss-Bonnet gravity". In: *Physical Review D* 99.4 (2019), p. 044017.

[69] Hayato Motohashi and Teruaki Suyama. "Third order equations of motion and the Ostrogradsky instability". In: *Physical Review D* 91.8 (2015), p. 085009.

[70] Yun Soo Myung and De-Cheng Zou. "Gregory-Laflamme instability of black hole in Einstein-scalar-Gauss-Bonnet theories". In: *Physical Review D* 98.2 (2018), p. 024030.

[71] Sh Nojiri, SD Odintsov, and VK3683913 Oikonomou. "Modified gravity theories on a nutshell: Inflation, bounce and late-time evolution". In: *Physics Reports* 692 (2017), pp. 1–104.

[72] Shin'Ichi Nojiri and Sergei D Odintsov. "Introduction to modified gravity and gravitational alternative for dark energy". In: *International Journal of Geometric Methods in Modern Physics* 4.01 (2007), pp. 115–145.

[73] Shin'ichi Nojiri, Sergei D. Odintsov, and Vasilis K. Oikonomou. "Ghost-free Gauss-Bonnet theories of gravity". In: *Physical Review D* (2018). URL: `https://api.semanticscholar.org/CorpusID:119062507`.

[74] Carlos Palenzuela et al. "Dynamical scalarization of neutron stars in scalar-tensor gravity theories". In: *Physical Review D* 89.4 (2014), p. 044024.

[75] Alexandre M Pombo and Daniela D Doneva. "Effects of mass and self-interaction on nonlinear scalarization of scalar-Gauss-Bonnet black holes". In: *Physical Review D* 108.12 (2023), p. 124068.

[76] Joel R. Primack. "Dark Matter and Structure Formation in the Universe". In: *arXiv: Astrophysics* (1997). URL: `https://api.semanticscholar.org/CorpusID:119430879`.

[77] Adam G Riess et al. "Observational evidence from supernovae for an accelerating universe and a cosmological constant". In: *The astronomical journal* 116.3 (1998), p. 1009.

[78] G Roepstorff. "Superconnections and the Higgs field". In: *Journal of Mathematical Physics* 40.6 (1999), pp. 2698–2715.

[79] Dalia Saha and Abhik Kumar Sanyal. "Inflation–a Comparative Study Amongst Different Modified Gravity Theories". In: *arXiv preprint arXiv:2201.02473* (2022).

[80] M Sami. "Models of dark energy". In: *The Invisible Universe: Dark Matter and Dark Energy*. Springer, 2007, pp. 219–256.

[81] Yu Shtanov, J Traschen, and RH1995PhRvD Brandenberger. "Universe reheating after inflation". In: *Physical Review D* 51.10 (1995), p. 5438.

[82] Hector O Silva et al. "Spontaneous scalarization of black holes and compact stars from a Gauss-Bonnet coupling". In: *Physical review letters* 120.13 (2018), p. 131104.

[83] Thomas P Sotiriou and Shuang-Yong Zhou. "Black hole hair in generalized scalar-tensor gravity: An explicit example". In: *Physical Review D* 90.12 (2014), p. 124063.

[84] Christian F Steinwachs. "Higgs field in cosmology". In: *One Hundred Years of Gauge Theory: Past, Present and Future Perspectives* (2020), pp. 253–287.

[85] Takashi Torii, Hiroki Yajima, and Kei-ichi Maeda. "Dilatonic black holes with a Gauss-Bonnet term". In: *Physical Review D* 55.2 (1997), p. 739.

[86] Slava G Turyshev. "Experimental tests of general relativity". In: *Annual Review of Nuclear and Particle Science* 58.1 (2008), pp. 207–248.

[87] L Arturo Ureña-López. "Brief review on scalar field dark matter models". In: *Frontiers in Astronomy and Space Sciences* 6 (2019), p. 47.

[88] Mariana Vargas-Magana et al. "Unraveling the Universe with DESI". In: *arXiv preprint arXiv:1901.01581* (2019).

[89] Volkov and Dmitry V. Galtsov. "NonAbelian Einstein Yang-Mills black holes". In: *Jetp Letters* 50 (1989), pp. 346–350. URL: `https://api.semanticscholar.org/CorpusID:116695718`.

[90] Clifford M Will. "The 1919 measurement of the deflection of light". In: *Classical and Quantum Gravity* 32.12 (2015), p. 124001.

[91] Clifford M Will. "The confrontation between general relativity and experiment". In: *Living reviews in relativity* 17.1 (2014), pp. 1–117.

[92] Richard P Woodard. "The theorem of Ostrogradsky". In: *arXiv preprint arXiv:1506.02210* (2015).

[93] Rui Xu, Yong Gao, and Lijing Shao. "Strong-field effects in massive scalar-tensor gravity for slowly spinning neutron stars and application to X-ray pulsar pulse profiles". In: *Physical Review D* 102.6 (2020), p. 064057.

[94] Ariel R Zhitnitsky. "Inflaton as an auxiliary topological field in a QCD-like system". In: *Physical Review D* 89.6 (2014), p. 063529.